



Towards Connecting the Remaining 3 Billion



Mohamed-Slim Alouini



Vehicle-to-everything



E-Health



Extended Reality



Super eMBB

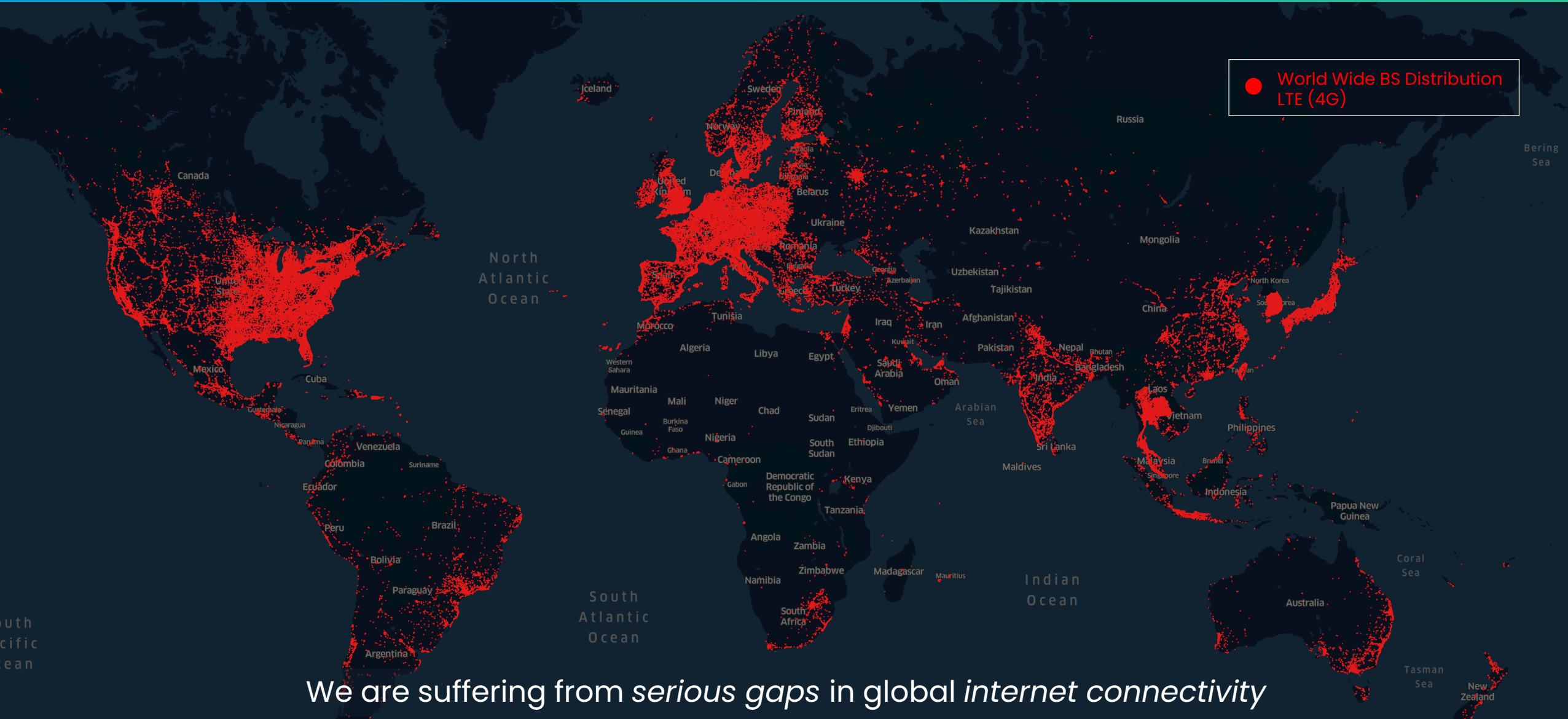


Artificial Intelligence



Industrial IoT



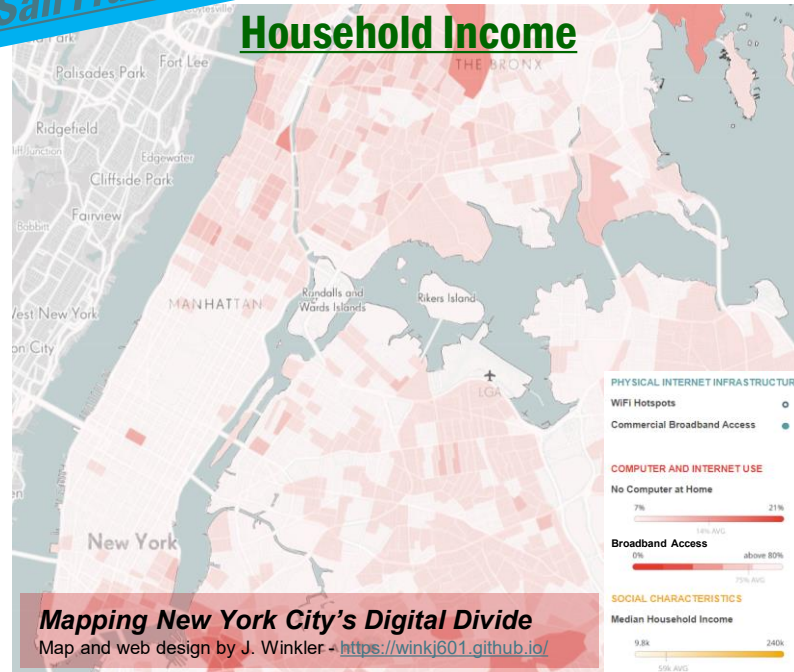


E. Yaacoub and M.-S. Alouini, "A Key 6G Challenge and Opportunity – Connecting the Base of the Pyramid: A Survey on Rural Connectivity", Proceedings of IEEE, 2020.

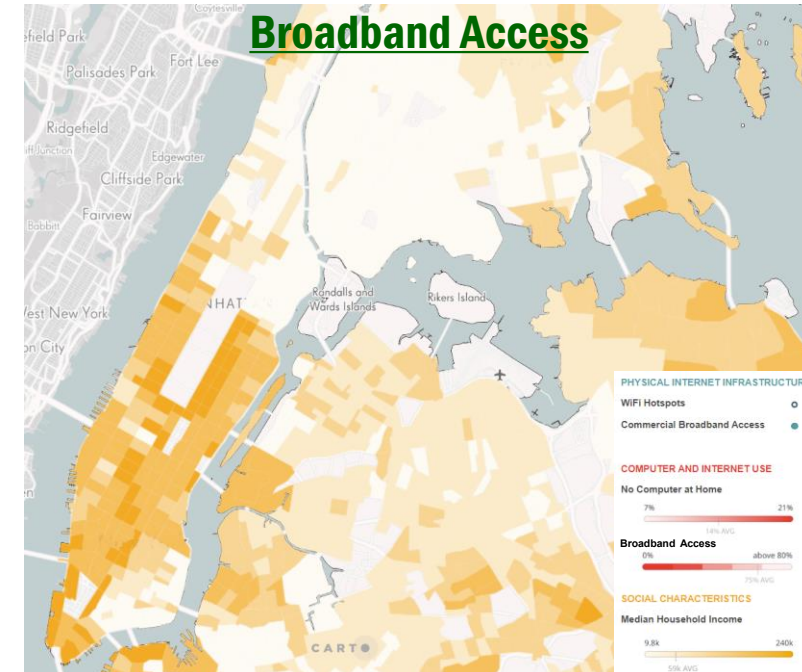
Digital Divide Is Wider Than We Think. **The New York Times**

The Former Homeless Man Bringing Web Access to the Bronx. **BBC**

Can San Francisco Finally Close its Digital Divide? **SF WEEKLY**



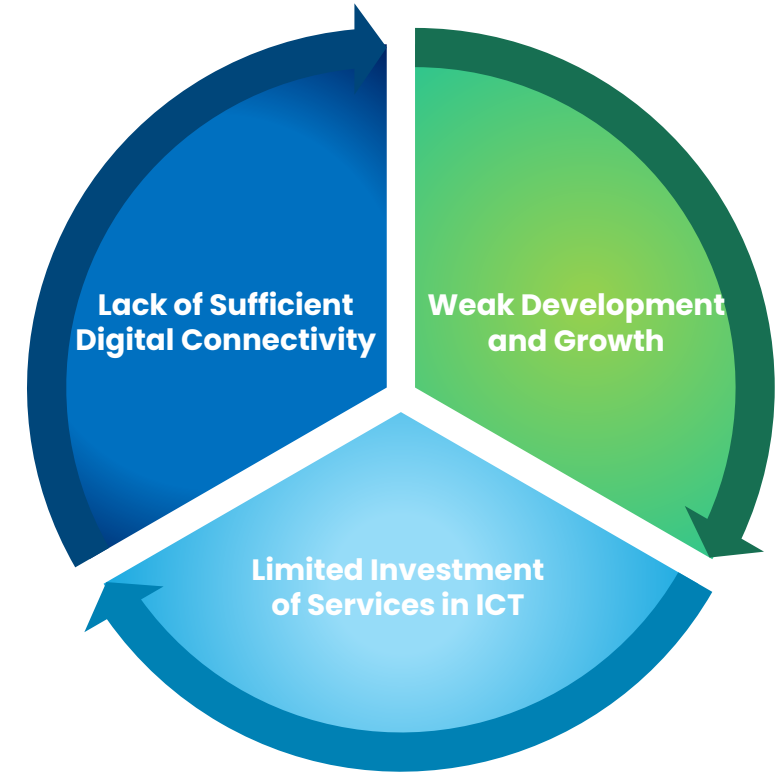
VS



- In communities with low income, the digital disparity is much more profound.
- People who have high-quality internet service are more likely to benefit from health care, self-education and social/governmental services.
- It needs collaboration and agreement among various stakeholders, i.e., government, policy makers, service provider, manufacturer and community members.



Cooperation
needed to bring
reliable internet
to those without it



**VICIOUS CYCLE of
DIGITAL DIVIDE**

Social Barriers

Poor infrastructure

**Low quality of education
for schooling**

Shortage of healthcare

The United Nations SDGs should **Drive** the evolution of 6G



6G should target



Improved
Energy Efficiency



No Bad Effects on **Environment** &
Human Health



More
Security and **Privacy**



Digital
Inclusion



Resilience, Robustness,
and **Dependability**

Disasters

Exploration

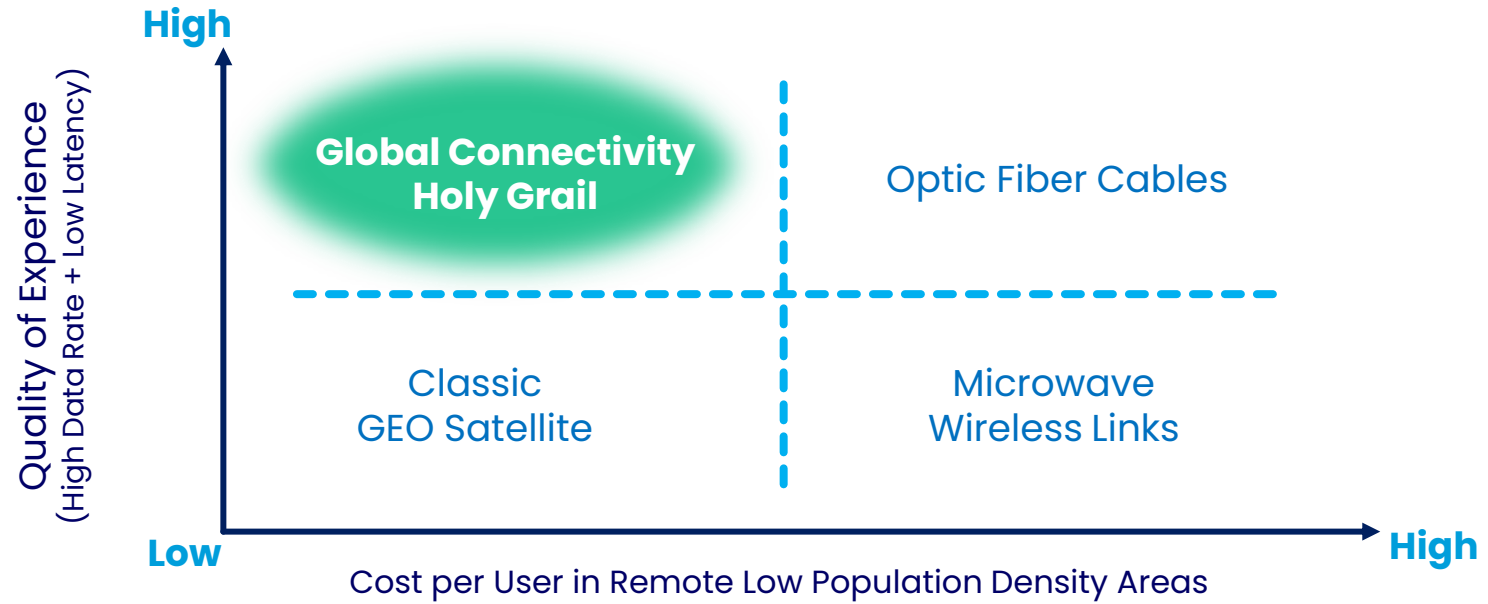
Military Mission

IoT Everywhere

Special Events

Urban Aerial
Mobility/Aeronautical

Maritime



A telephone subscriber here may call up and talk to any other subscriber on the **Globe**. An **inexpensive** receiver, not bigger than a watch, will enable him to listen **anywhere**, on **land** or **sea**, to a speech delivered or music played in some other place, however **distant**.

— Nikola Tesla 1919

Manufacturing Cost Down => Mass Production



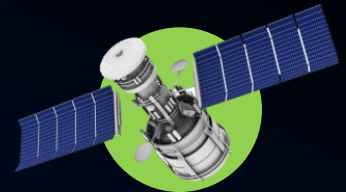
Geostationary Earth Orbit (GEO) Satellite

- Fixed position in the sky at ~35,000 km
- Relatively large delay
- ViaSat 1, 2, 3



Medium Earth Orbit (MEO) Satellite

- 2,000~35,000 km
- Position and tracking
- O3B, SES Networks



Low Earth Orbit (LEO) Satellite

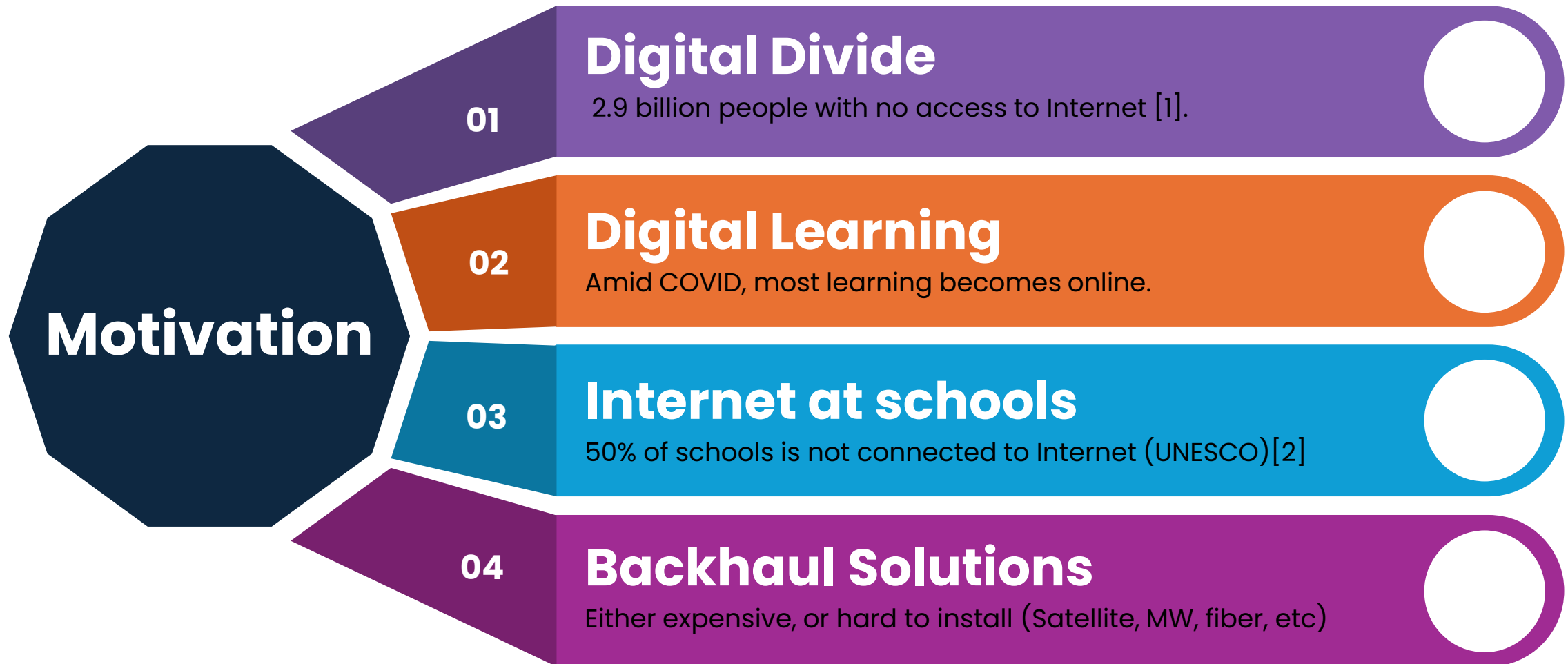
- 160~2,000 km
- Hand-Over
- OneWeb, Starlink, Lightspeed, Kuiper, GW, G60





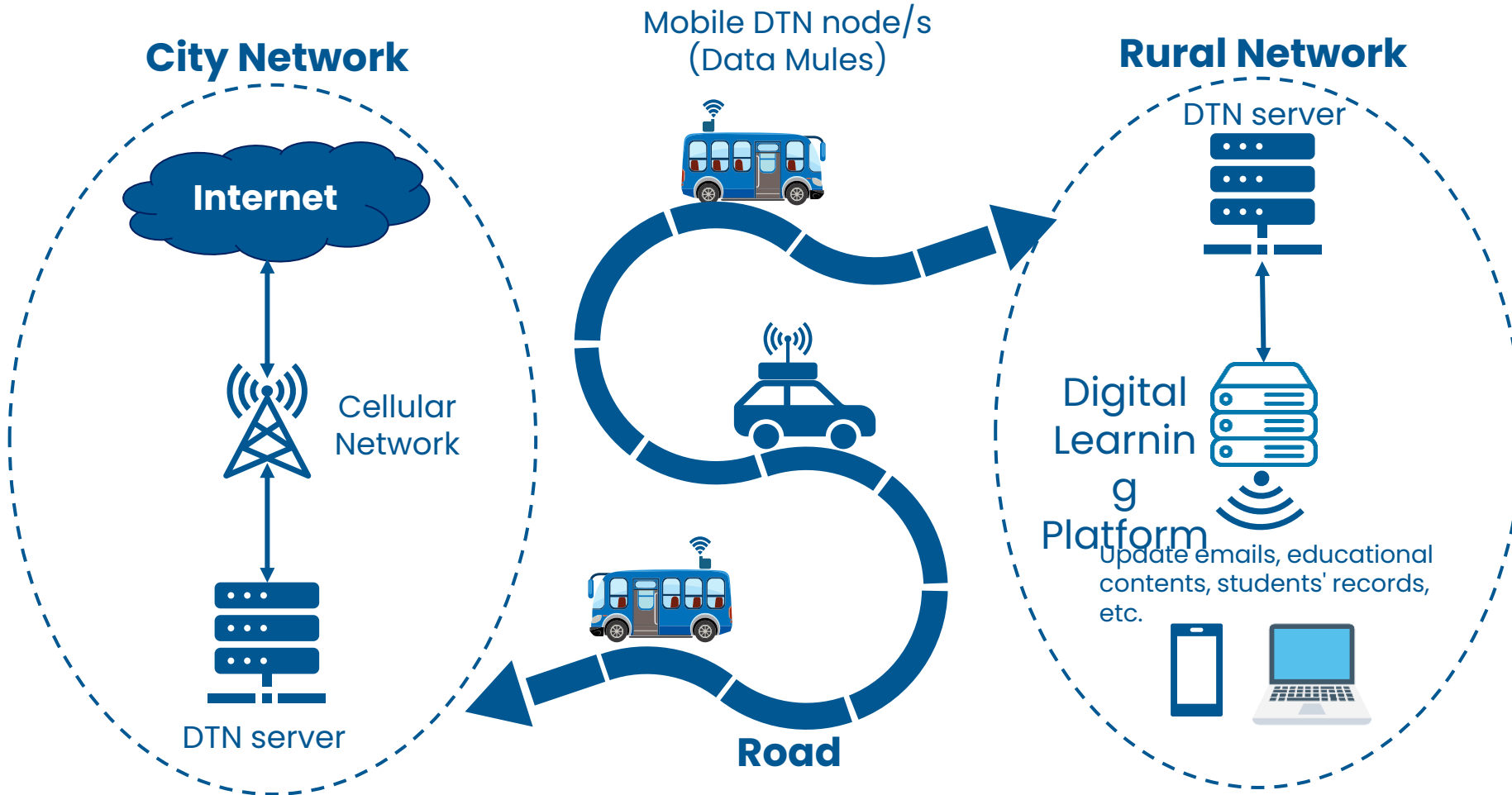
Bridging the Educational Divide: A Delay-Tolerant Networking Approach for Equitable Digital Learning in Rural Areas*

[*] S. Abdeljabar, and M-S. Alouini: "Bridging the Educational Divide: A Delay-Tolerant Networking Approach for Equitable Digital Learning in Rural Areas". *IEEE Technology and Society Magazine*, under review.

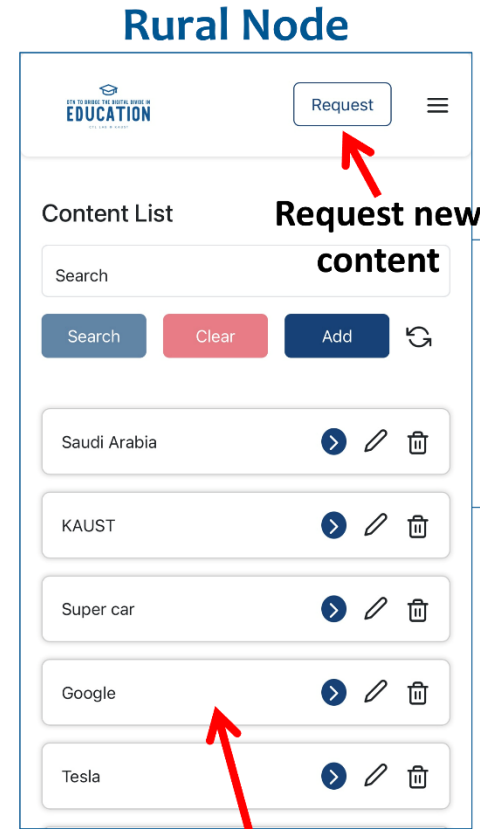
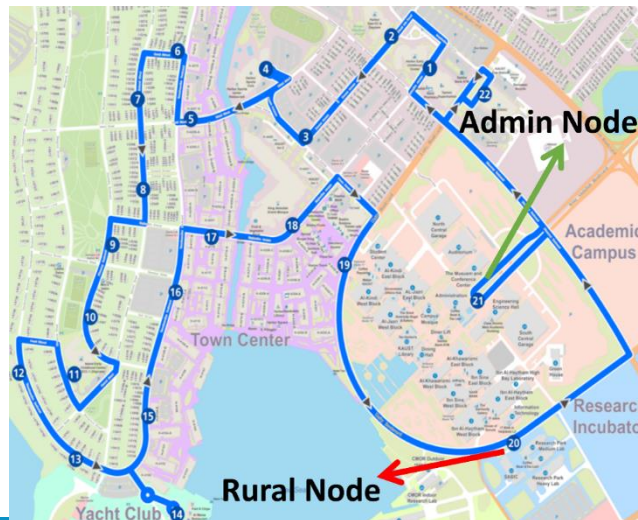
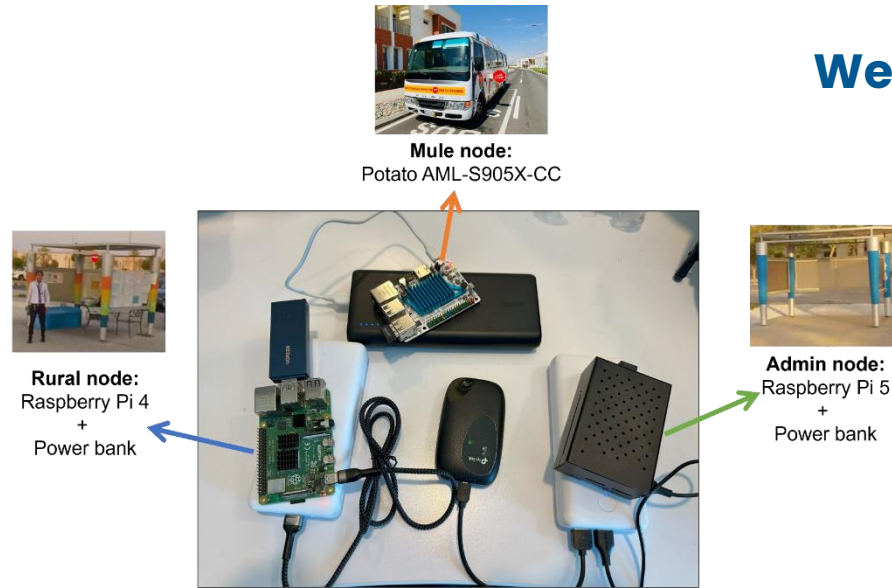


[1] "Global connectivity report - ITU," Apr 2023. [Online]. Available: <https://www.itu.int/hub/publication/d-ind-global-01-2022/>

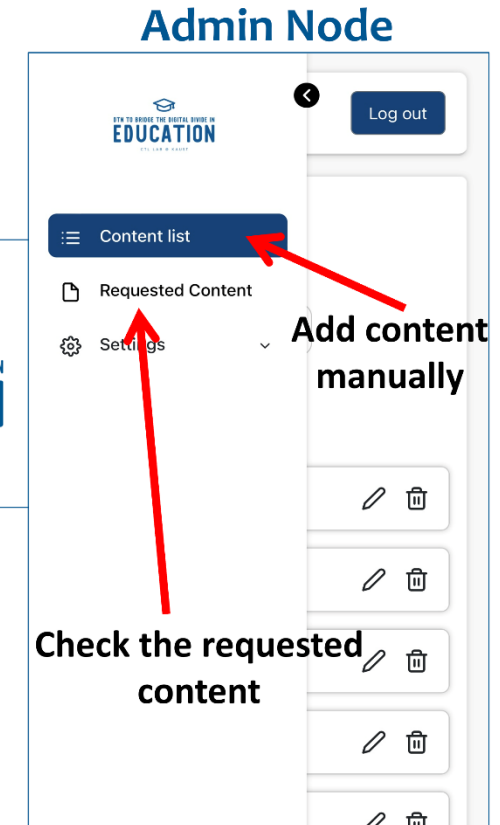
[2] "Secretary-general's report on "our common agenda", 2021. [Online]. Available: <https://www.un.org/en/content/common-agenda-report>



We designed and built a proof of concept for this system:

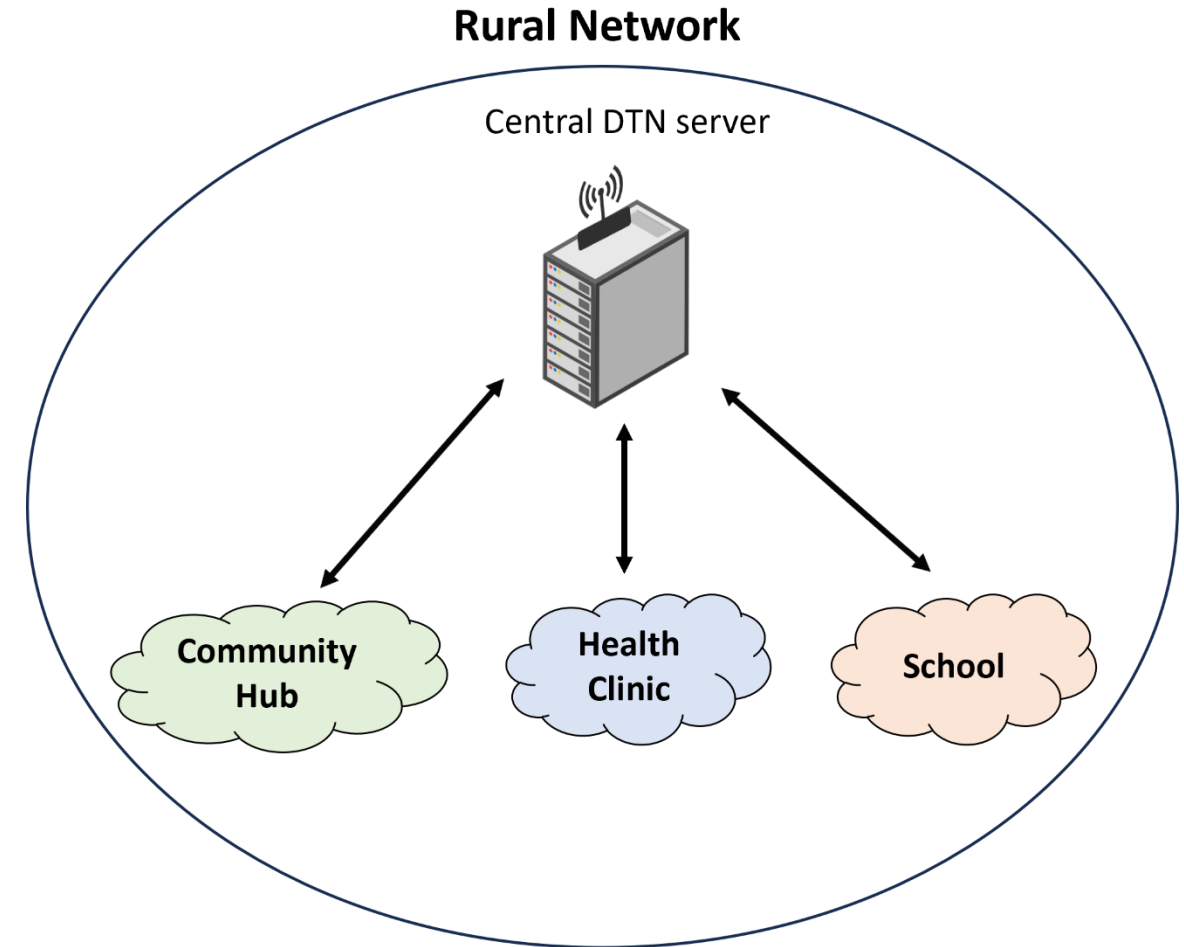


Read and modify available content



Application Logo

- Demonstrated a viable approach for digital learning in rural areas with limited or no internet access.
- DTN provides a cost-effective, backhaul-like solution for delivering educational content in remote regions.
- Initial tests on a campus bus using off-the-shelf components showed promising results for text-based content delivery.
- Planned improvements to support multimedia content and support broader community services and connectivity, increasing the system's impact.

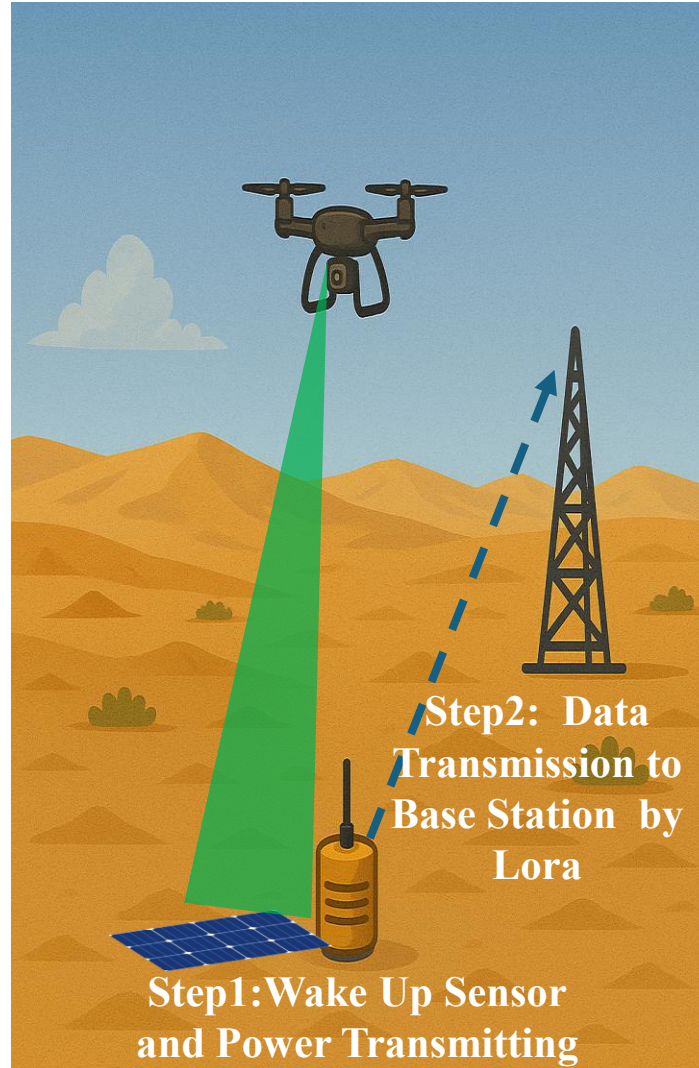




Laser-Based Wake-Up and Wireless Power Transfer

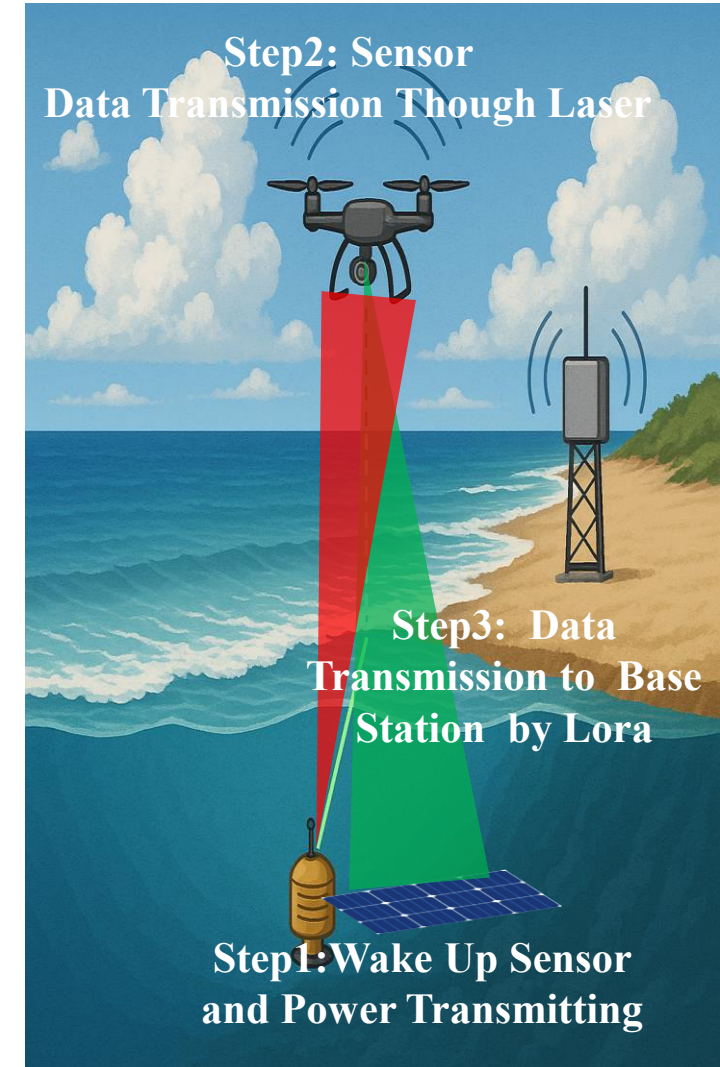
Remote Terrestrial Environments

- Step1: UAV transmits laser energy to wake up and power the ground sensor.
- Step2: The sensor sends collected data to the base station via LoRa.



Underwater Environments

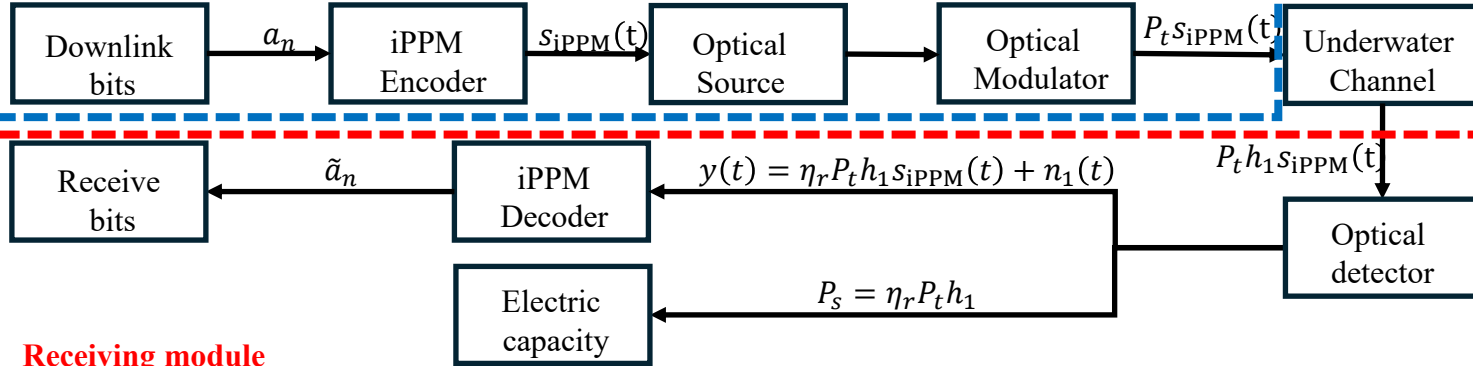
- Step 1: UAV delivers laser energy through the water to power the underwater sensor.
- Step 2: Sensor transmits data optically to the UAV.
- Step 3: UAV forwards data to the shoreline base station via LoRa.



Principle and Implementation

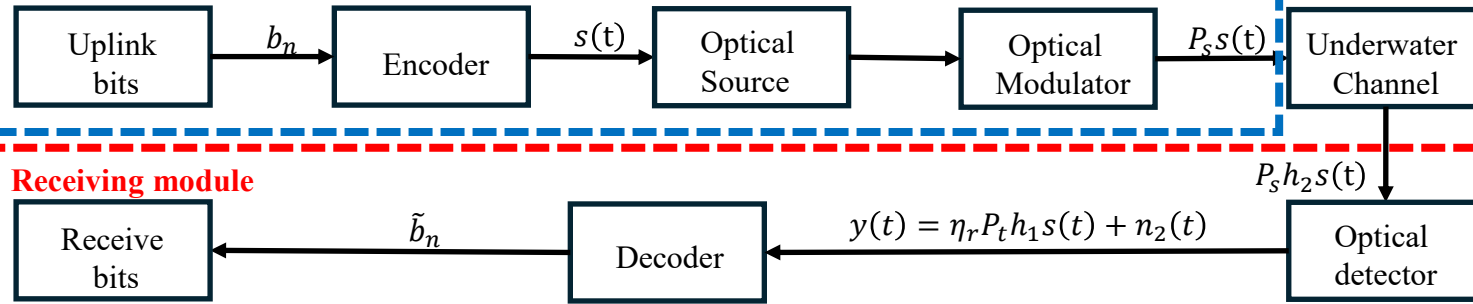
Step1: Wake Up Sensor

Transmitter module

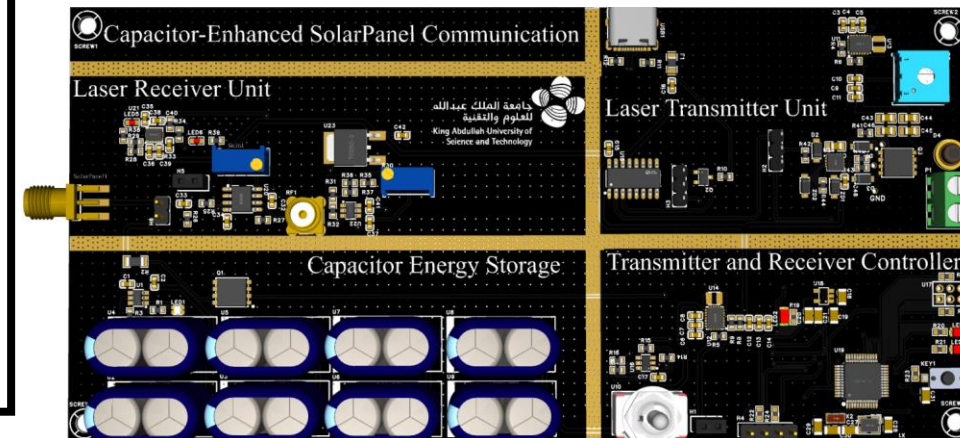


Step2: Sensor Data Transmission

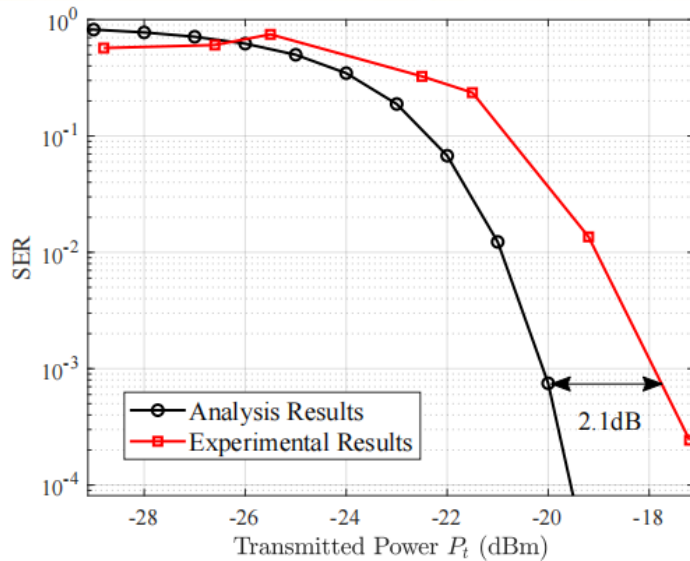
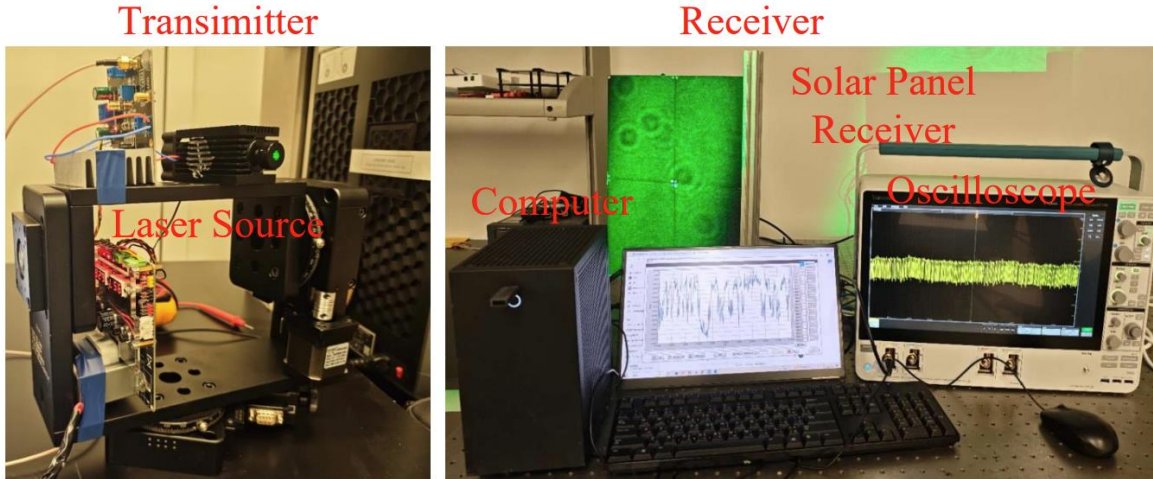
Transmitter module



Component	Description
Laser Source	530 nm diode laser, Output power 10 W
Beam Collimator	Lens-based, beam divergence < 2 mrad
Modulation	iPPM
MCU	STM32
Solar Panel (Rx)	efficiency $\sim 20\%$
Wake-Up Power	-20dBm
Lora Module	range > 2 km (LOS)



Indoor experiments ~3m



Laser Output Power	Electrical Power Output
1 W	0.14 W
2 W	0.28 W
4 W	0.56 W
5 W	0.70 W

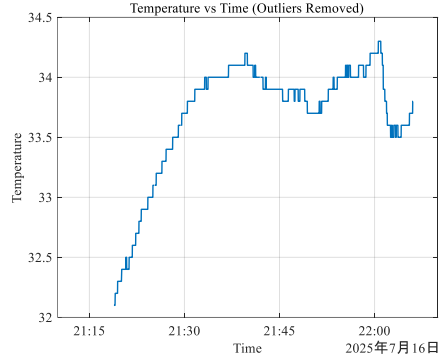
Outdoor experiments ~5km



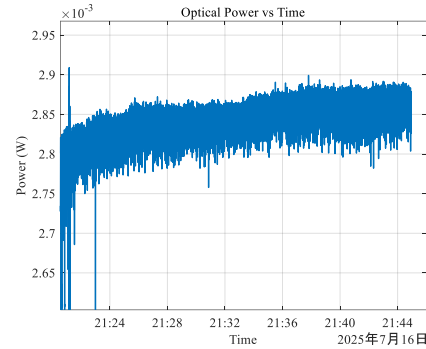
Paper:

[1] Z. Shi, Y. Zhang, J. Xu, and M.-S. Alouini, "Design and performance analysis of a UAV based capacitor-enhanced solar panel communication system," *Under Review*.

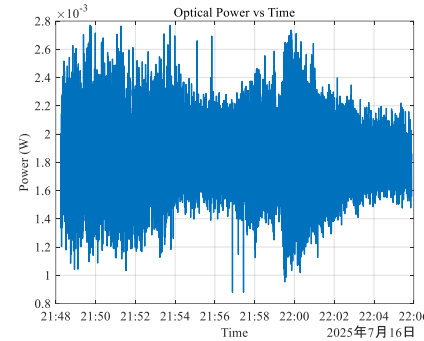
Outdoor experiments ~600m



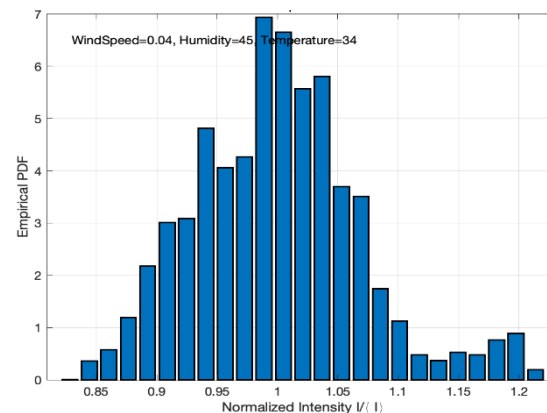
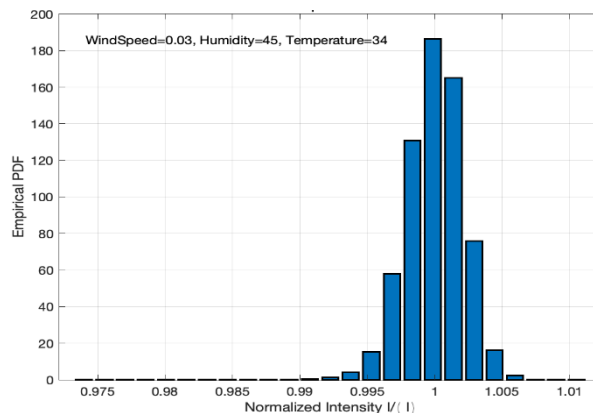
Temperature



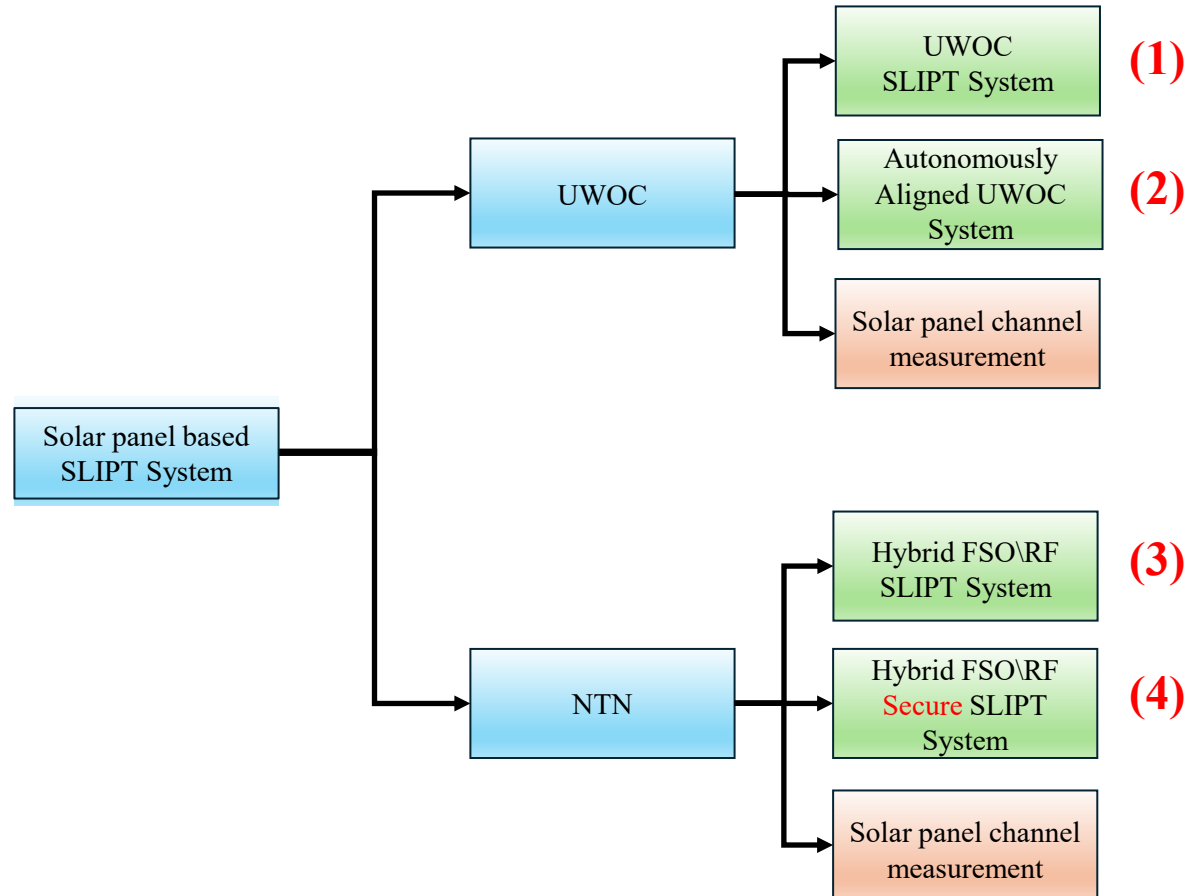
30cm X 20 cm
Solar Panel



6cm X 6 cm
Solar Panel



Larger solar panels (30cm × 20cm) demonstrate better resistance to atmospheric turbulence compared to smaller ones.





UNESCO
Chair on Education
Connect the Unconnected



جامعة الملك عبد الله
للعلوم والتقنية
King Abdullah University of
Science and Technology

UWOC-SLIPT System (1)



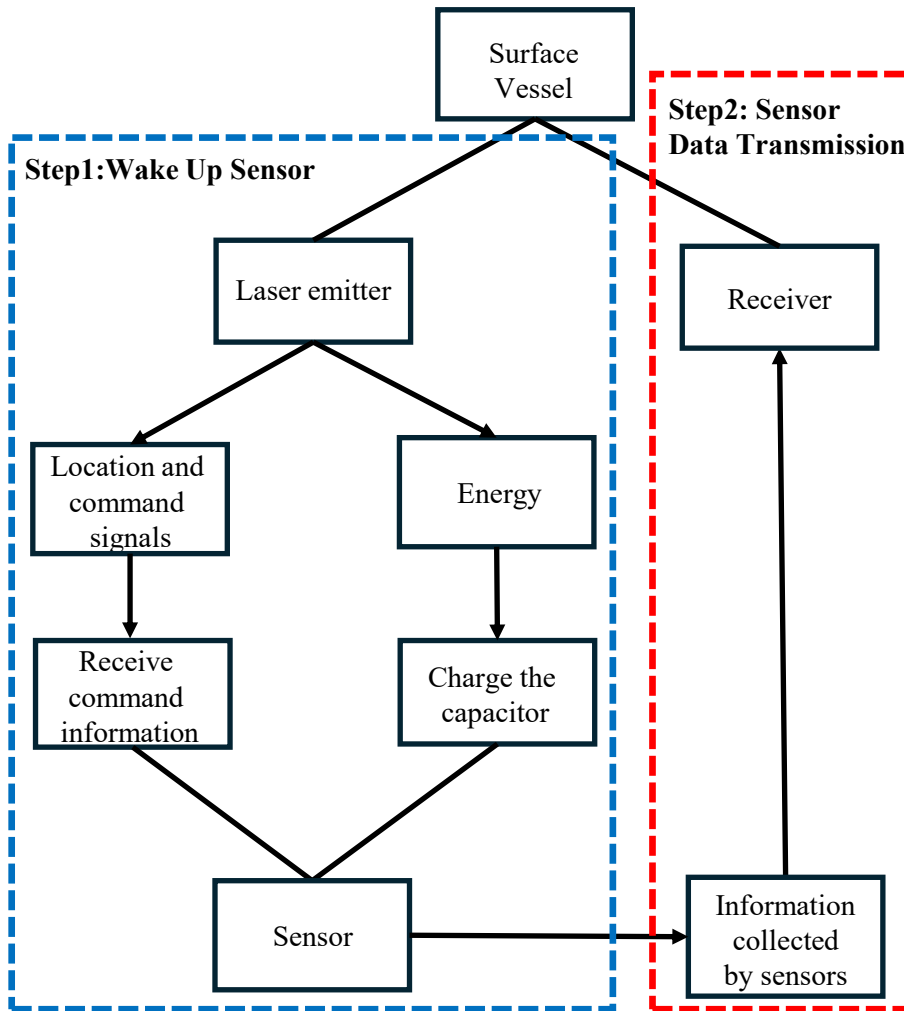


Fig.1 Workflow of Step 1–2: Wake Up → Charge → Data Uplink

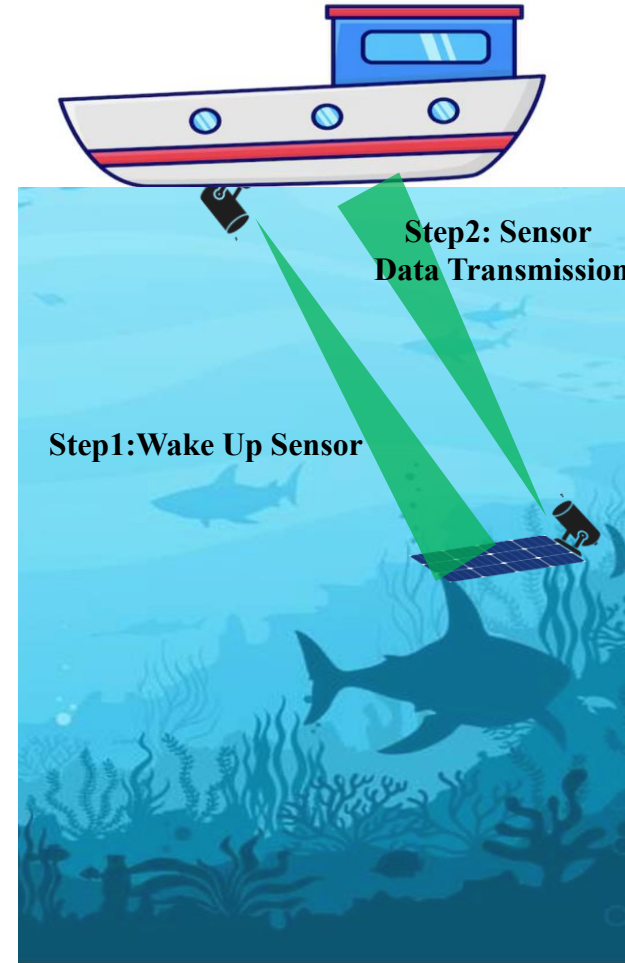


Fig.2 Application Scenario

Underwater communication,
RF is not a good option,
so our uplink also applies FSO

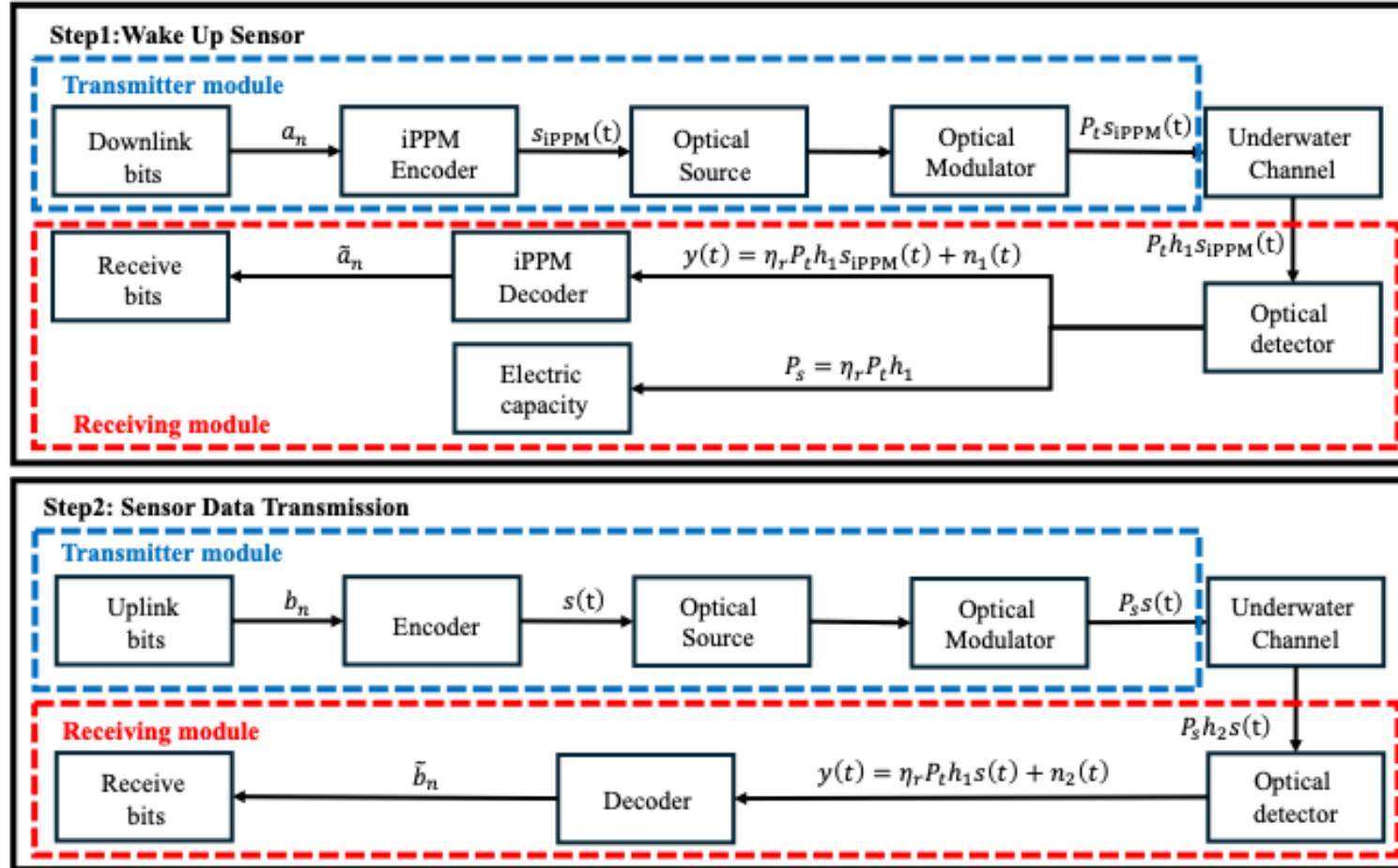


Fig.1 Two-phase SLIPT architecture for an underwater sensor

The transmission power is increased
M times compared to PPM.

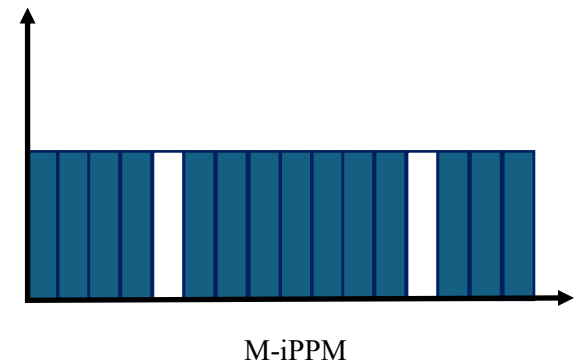
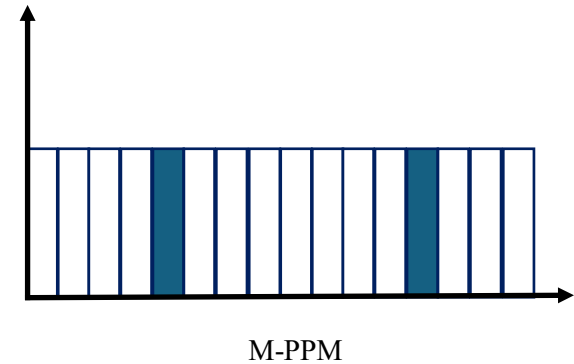


Fig.2 M-PPM vs. M-iPPM symbol patterns
(duty-cycle and average-power comparison).

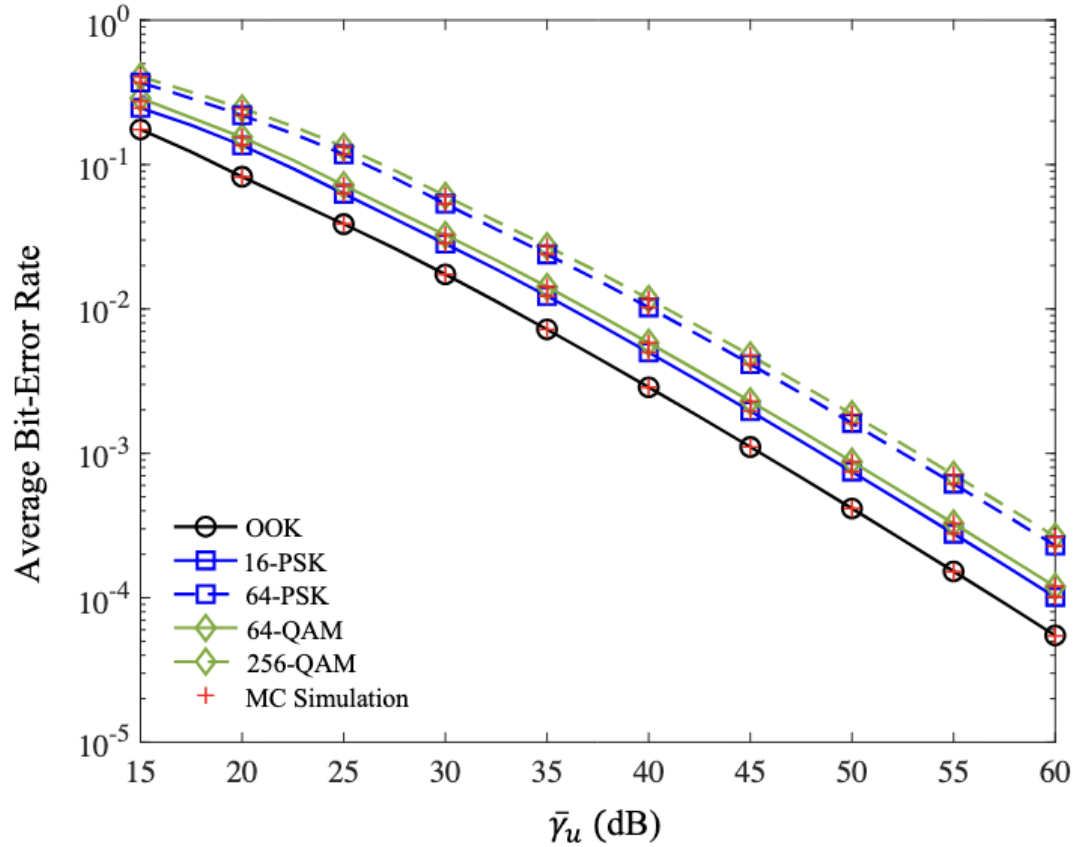


Fig. 1 Average BER versus average uplink SNR $\bar{\gamma}_u$ under various modulation schemes.

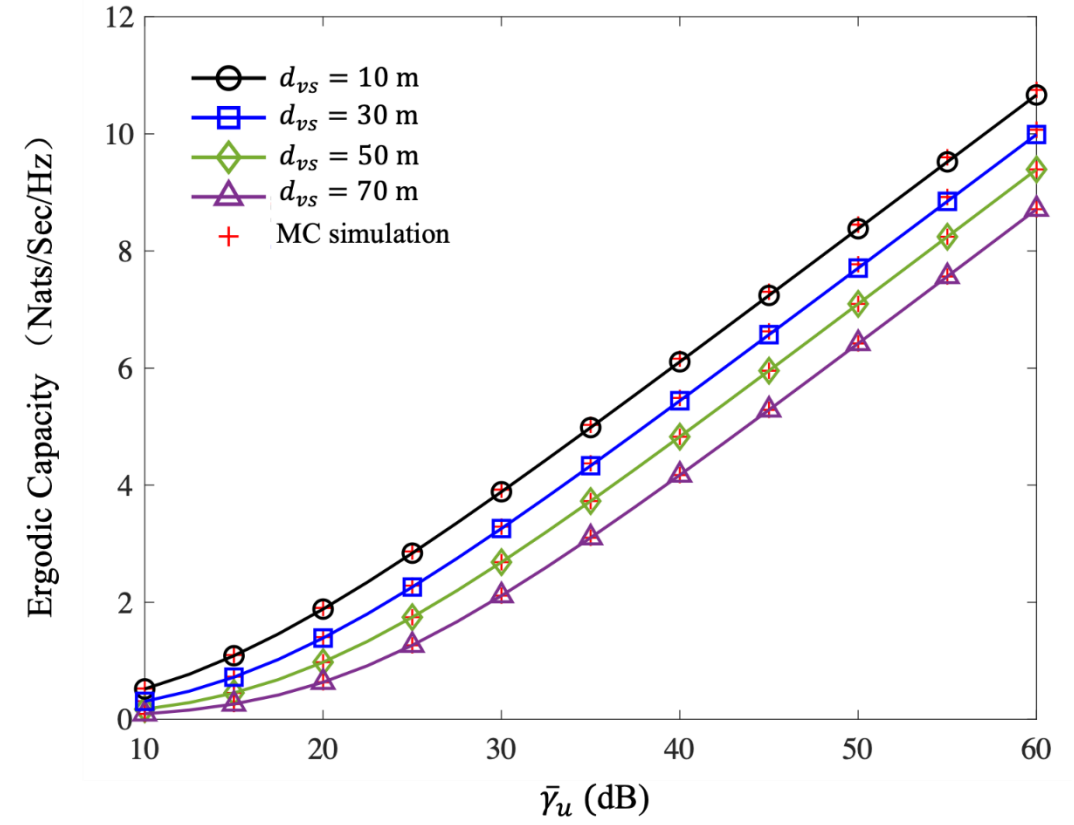


Fig. 2 Ergodic capacity versus average uplink SNR $\bar{\gamma}_u$ under different vertical distances d_{vs} .



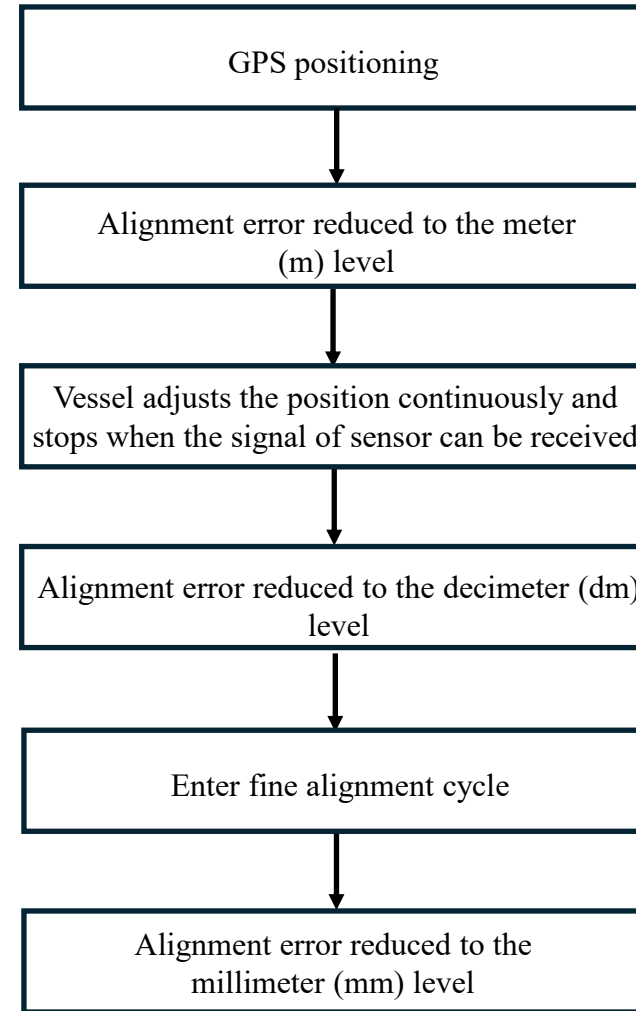
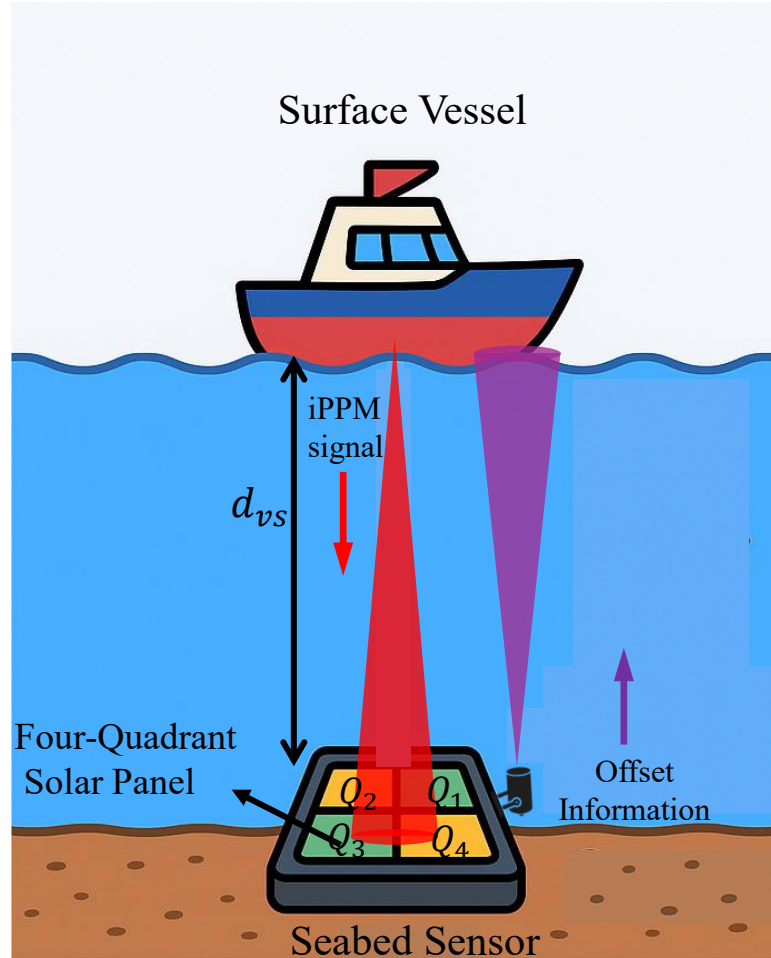
UNESCO

Chair on Education
Connect the Unconnected



جامعة الملك عبد الله
للعلوم والتقنية
King Abdullah University of
Science and Technology

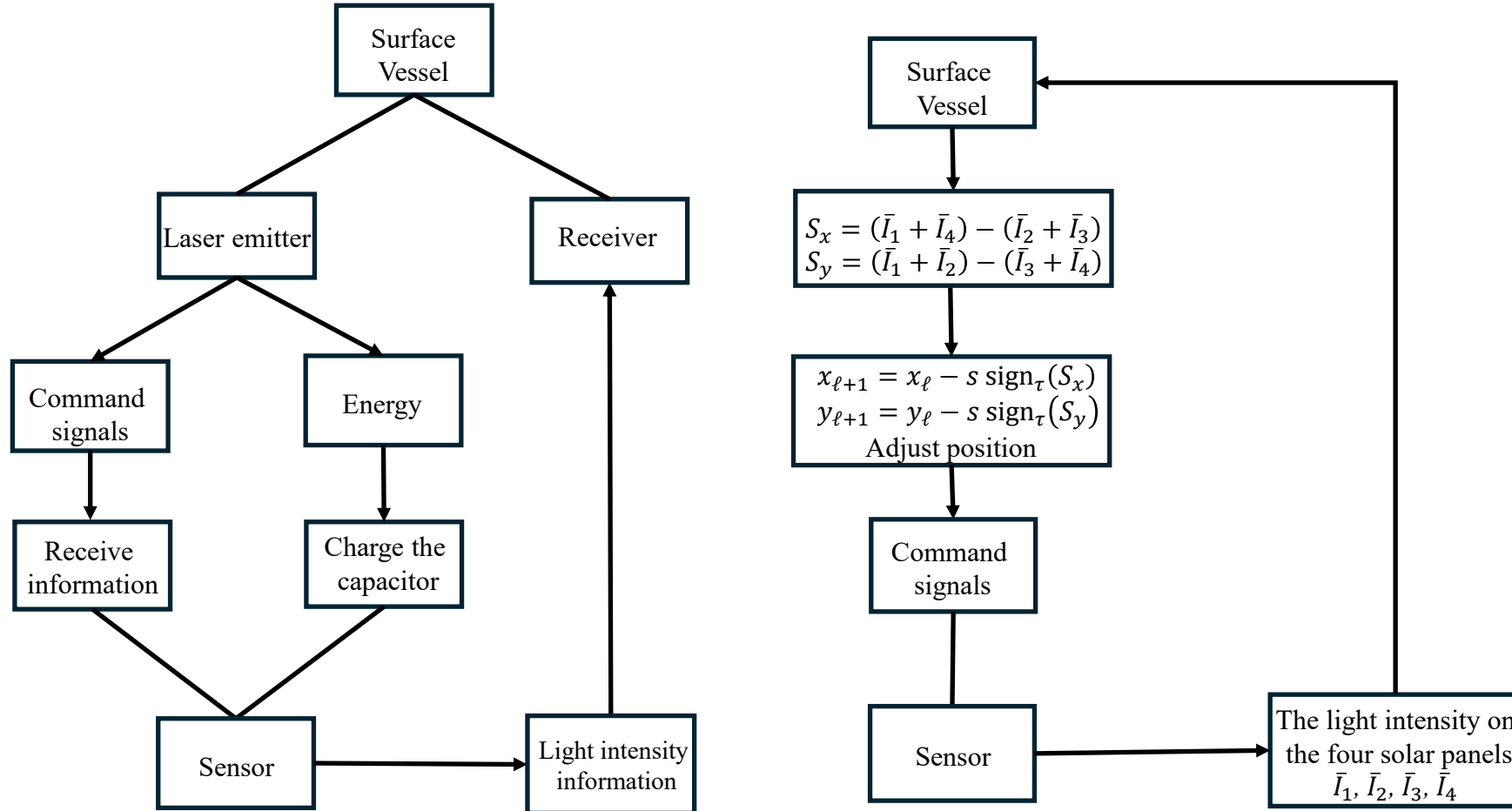
Autonomously Aligned UWOC System (2)



The biggest problem with underwater optical communication is **alignment**.

Traditional FSO communication uses a camera for alignment, which is too **costly**.

Fig.1 Coarse-to-fine optical alignment for underwater SLIPT

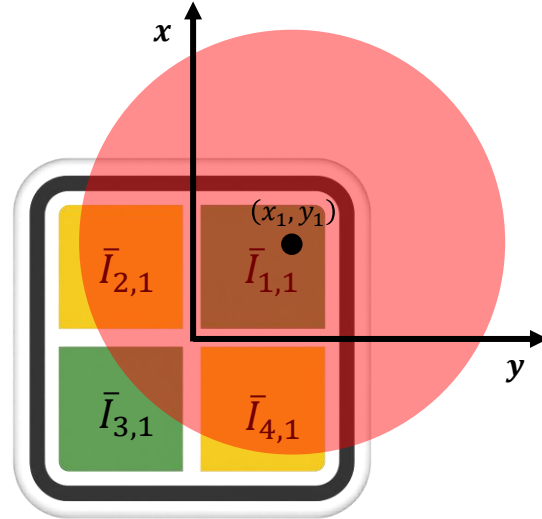
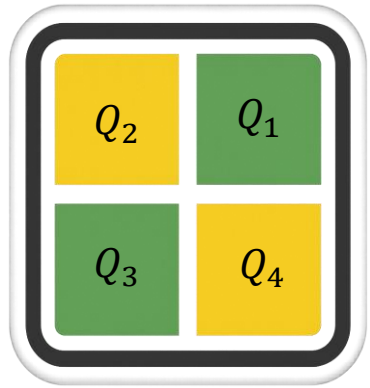


$$\text{sign}_\tau(x) = \begin{cases} 1, & x > \tau \\ 0, & \text{others} \\ -1, & x < \tau \end{cases}$$

τ is a dead-zone threshold introduced to suppress noise-induced actuation.

s denotes the fixed step size of the vessel.

Fig.1 Closed-loop alignment using four-quadrant intensity feedback.

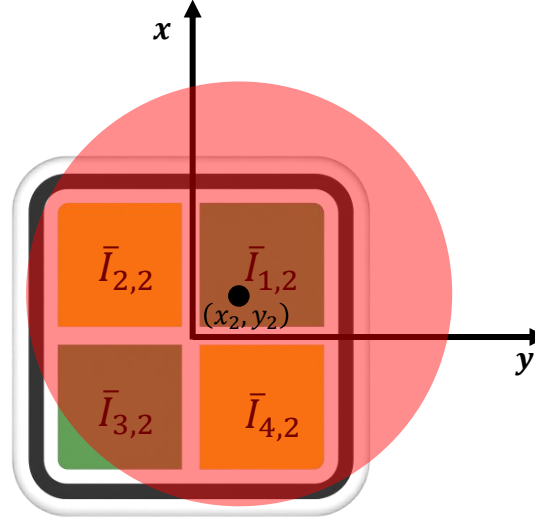


$$S_{x,1} = (\bar{I}_{1,1} + \bar{I}_{4,1}) - (\bar{I}_{2,1} + \bar{I}_{3,1})$$

$$S_{y,1} = (\bar{I}_{1,1} + \bar{I}_{2,1}) - (\bar{I}_{3,1} + \bar{I}_{4,1})$$

$$x_2 = x_1 - s \operatorname{sign}_\tau(S_{x,1})$$

$$y_2 = y_1 - s \operatorname{sign}_\tau(S_{y,1})$$

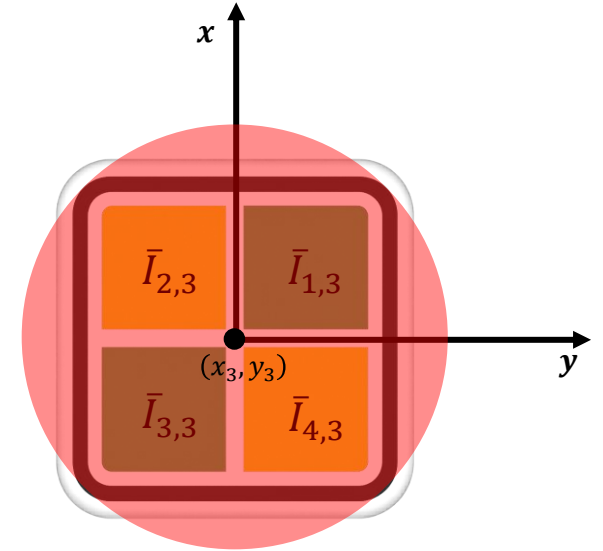


$$S_{x,2} = (\bar{I}_{1,2} + \bar{I}_{4,2}) - (\bar{I}_{2,2} + \bar{I}_{3,2})$$

$$S_{y,2} = (\bar{I}_{1,2} + \bar{I}_{2,2}) - (\bar{I}_{3,2} + \bar{I}_{4,2})$$

$$x_3 = x_2 - s \operatorname{sign}_\tau(S_{x,1})$$

$$y_3 = y_2 - s \operatorname{sign}_\tau(S_{y,1})$$



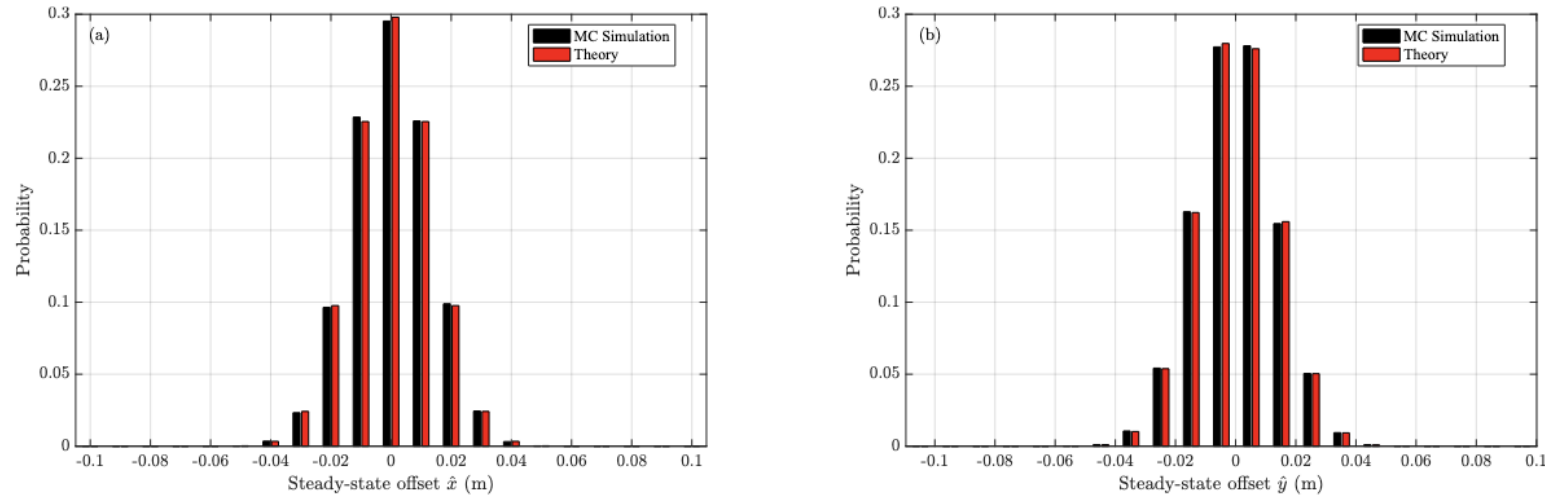


Fig. 1 Marginal steady-state offset distributions for (a) \hat{x} and (b) \hat{y} , comparing MC simulation (black) with the closed-form theory (red).

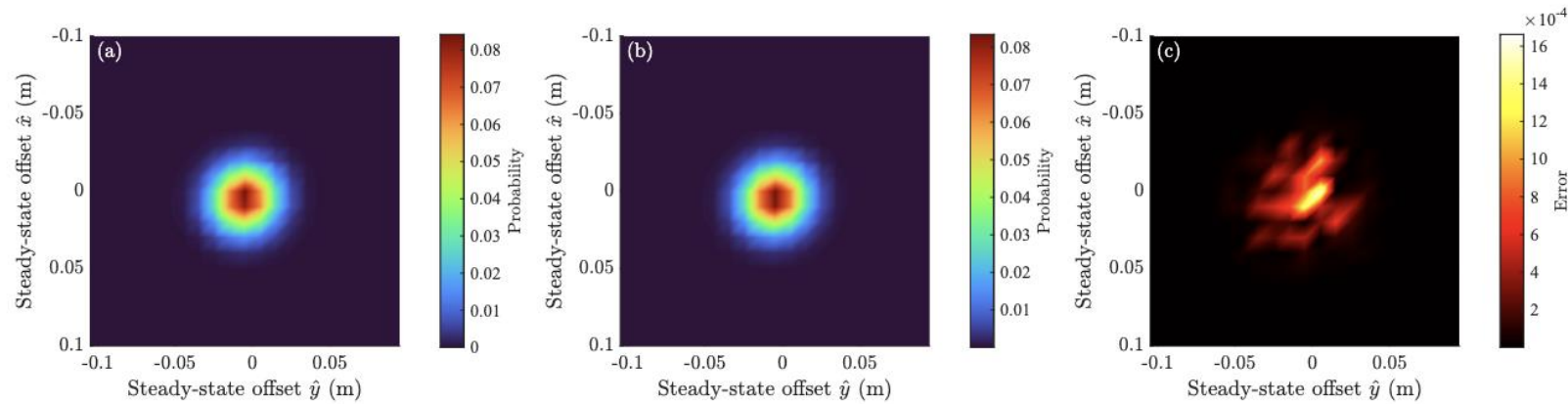


Fig. 2 Two-dimensional joint probability surfaces over the discrete state grid: (a) simulation, (b) theoretical, and (c) absolute error.



UNESCO

Chair on Education
Connect the Unconnected



جامعة الملك عبد الله
للعلوم والتقنية
King Abdullah University of
Science and Technology

SLIPT Hybrid FSO/RF System (3)



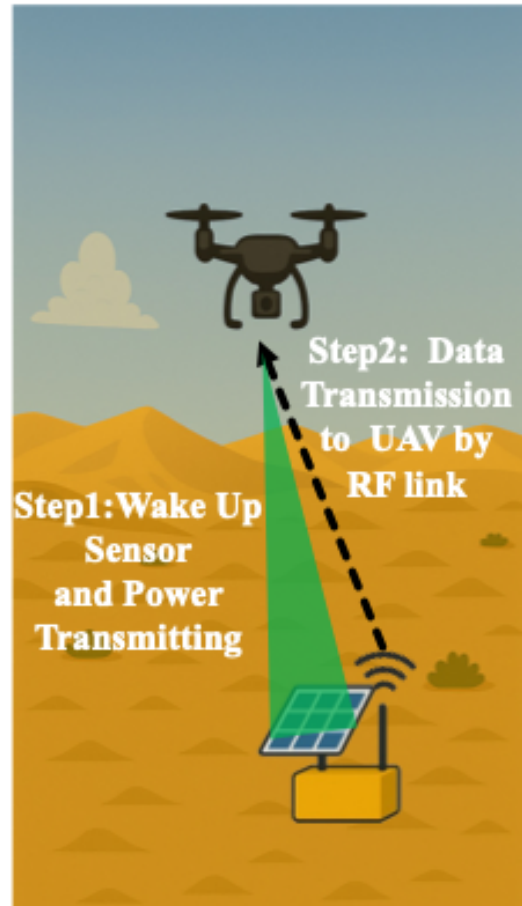


Fig.1 Application Scenario

In ground communication, RF has more advantages than FSO.

1. Wide range of coverage
2. low energy consumption

However, RF may have the issue of information leakage.

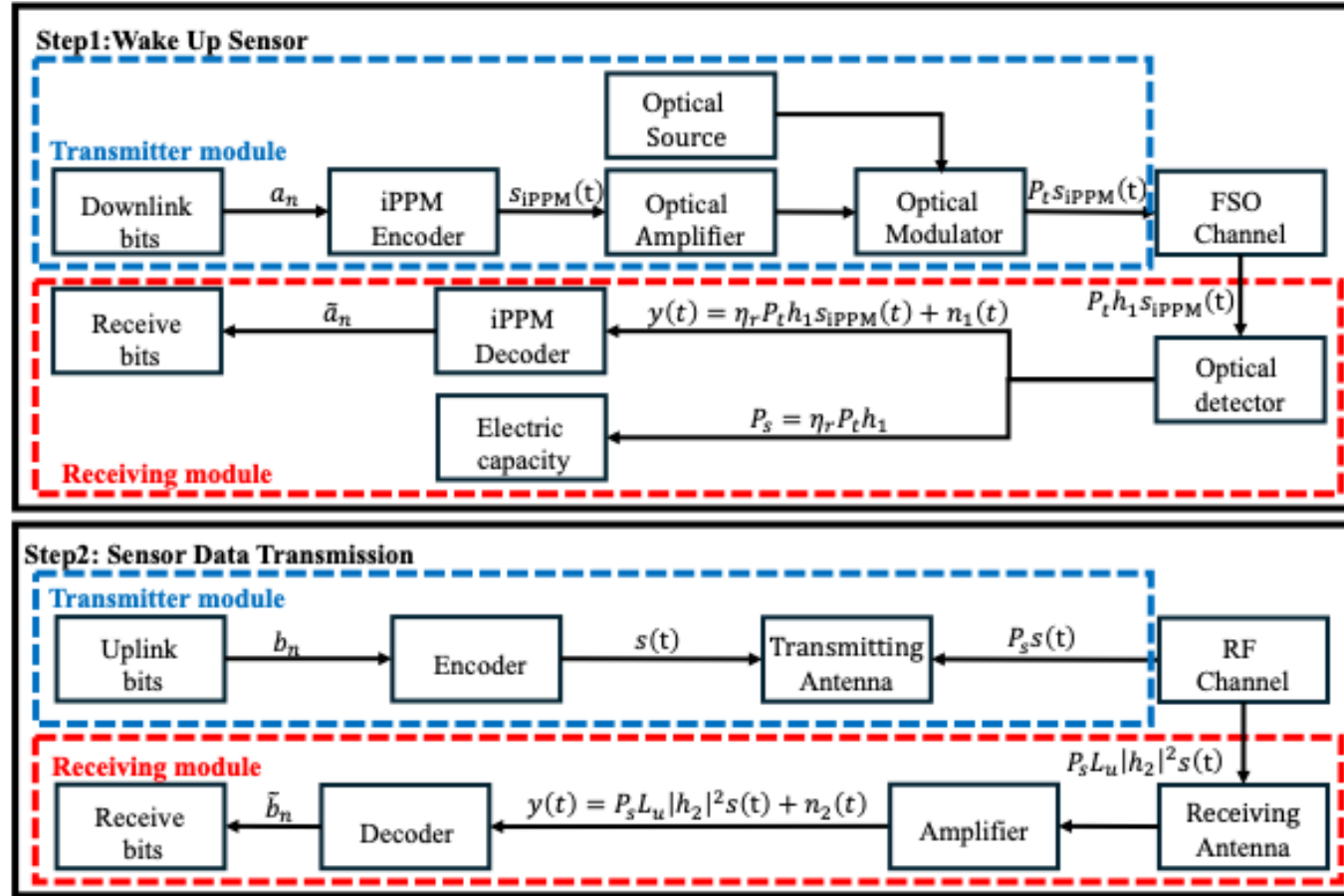


Fig.1 Two-phase SLIPT architecture

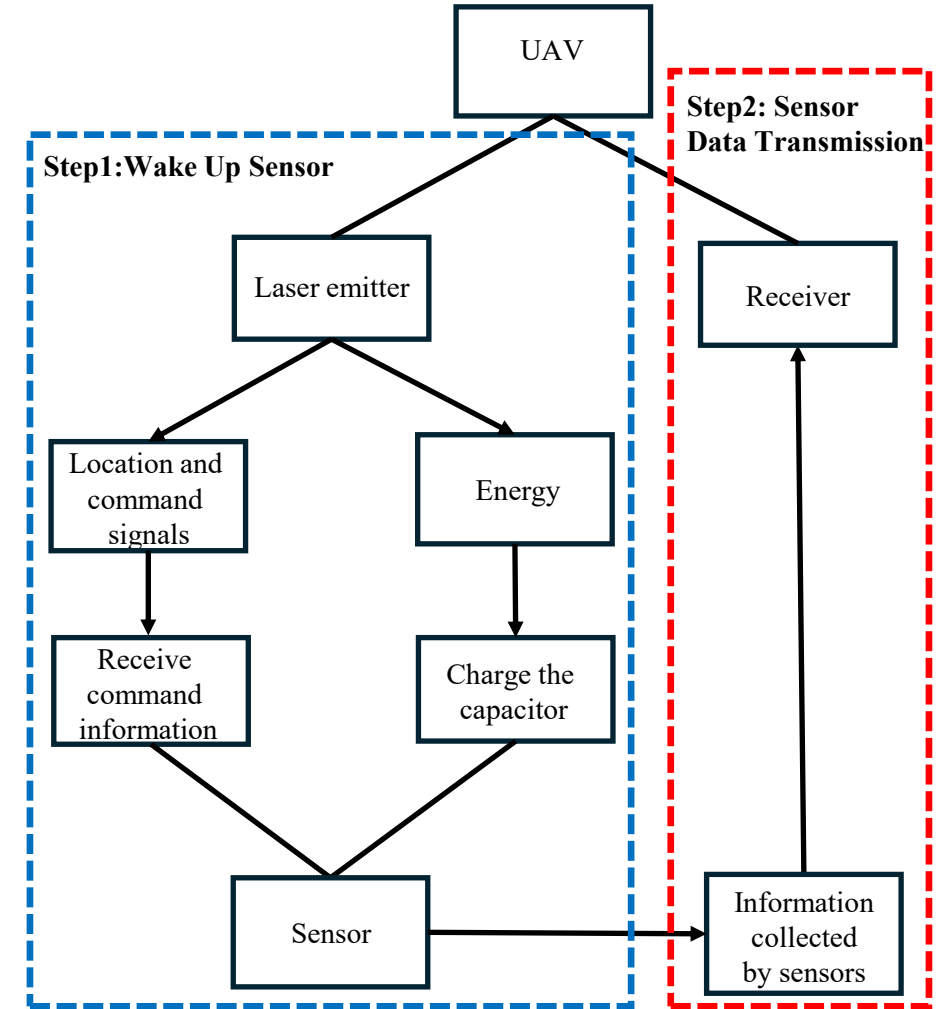


Fig.2 Workflow of Step 1-2: Wake Up → Charge → Data Uplink



UNESCO

Chair on Education
Connect the Unconnected



جامعة الملك عبد الله
للعلوم والتقنية
King Abdullah University of
Science and Technology

Secure SLIPT Hybrid FSO/RF System (4)

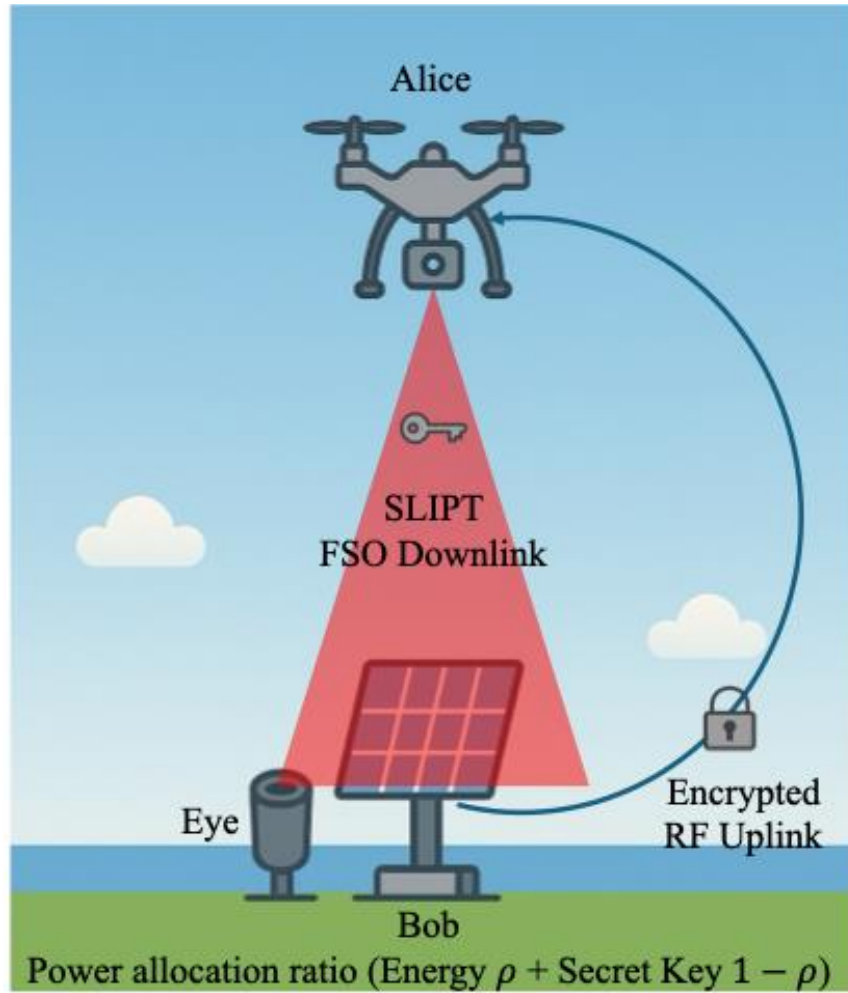


Fig.1 Application Scenario

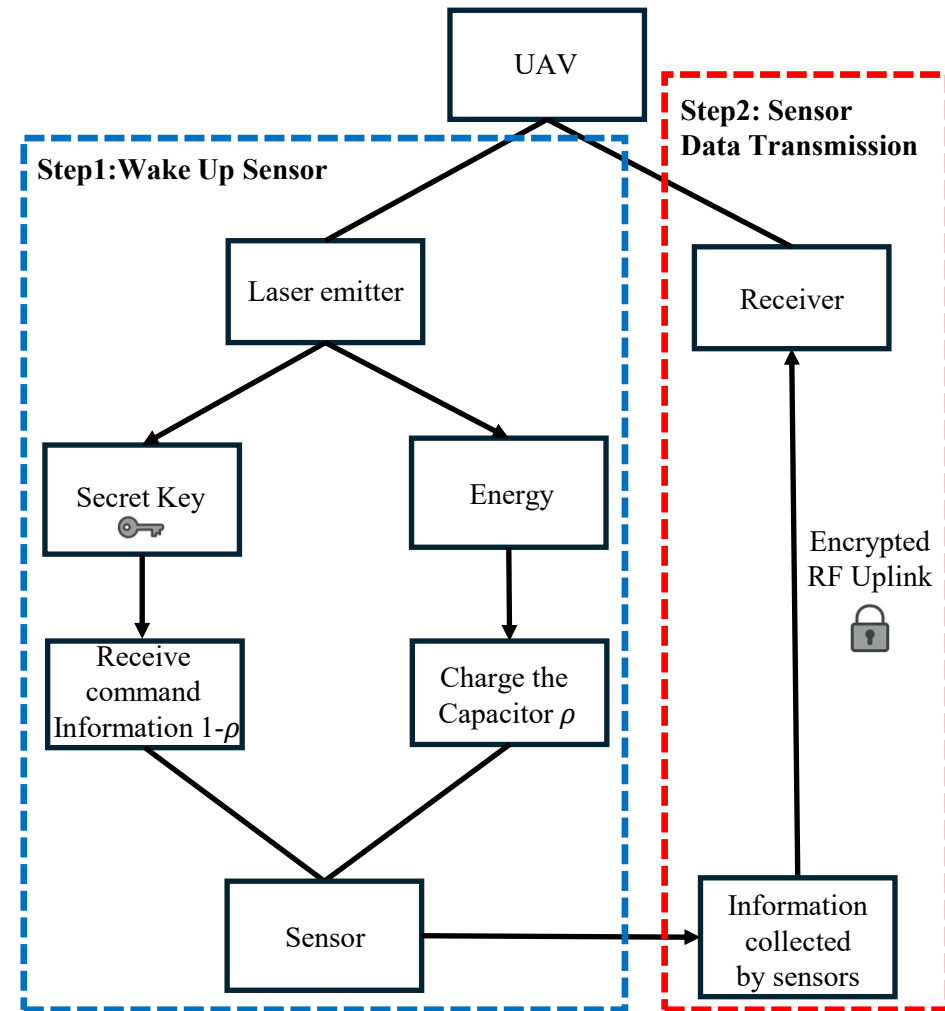


Fig.2 Workflow of Step

$$\text{Secret capacity: } C_s = [C_b - C_e]^+$$

$$\text{Secret Outage Probability: SOP} = \mathbb{P}(C_s > C_{th})$$

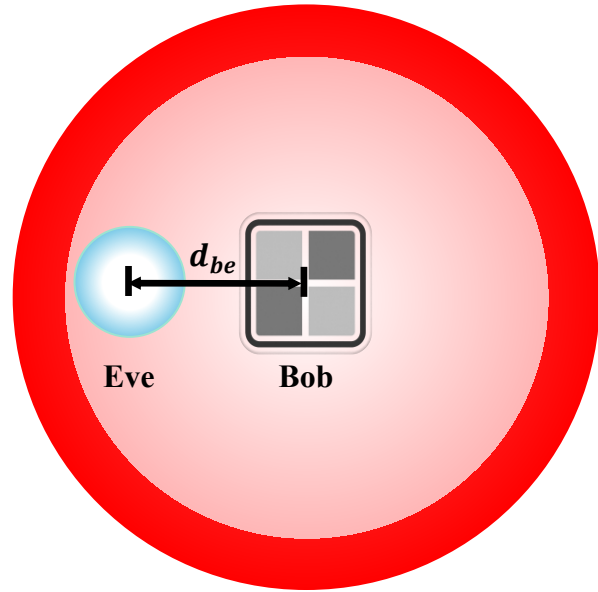


Fig.1 Application Scenario

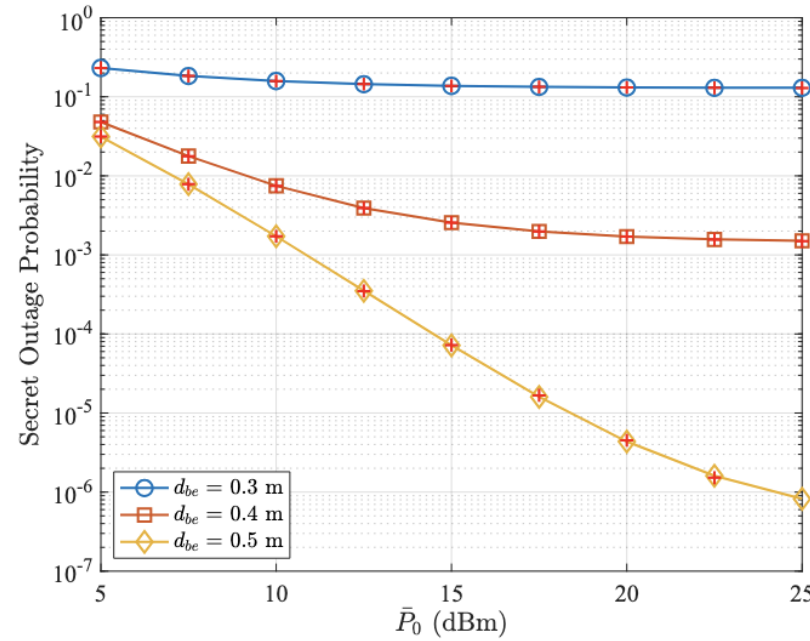


Fig. 2. SOP versus average optical transmit power \bar{P}_0 under different sensor-Eye separation distances d_{be} with $\omega_b = 5r_a$.

$$\text{Secret Coverage Probability: } P_c = 1 - \text{SOP}$$

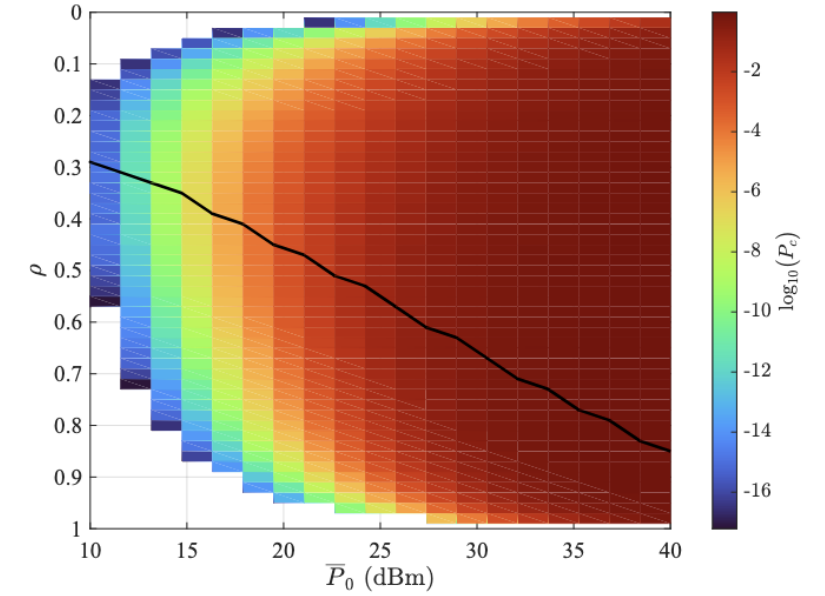


Fig. 3 Heatmap of the logarithmic CP $\log_{10}(P_c)$ versus average optical transmit power P_0 and power splitting ratio ρ . The black curve indicates the optimal ρ^* that maximizes P_c for each \bar{P}_0 .

◆ Background

- NASA's TBIRD program successfully demonstrated > 100 Gbps link from a single CubeSat to the ground, which can be utilized in delay-tolerant networks (DTNs) for high-volume data transmission from LEO to Earth [1].
- Advantages of single-satellite system: Low computational and hardware complexity, reduced size, weight, and power (SWaP) requirements.
- Using free space optical (FSO) links overcomes traditional RF limitations.

◆ Motivation

- The DTN paradigm enables satellites to store data when out of contact and forward it during visibility windows, providing greater reliability.
- Satellite ergodic capacity performance is governed by orbital geometry.
- LEO satellites operate between 160–2,000 km altitude [2]

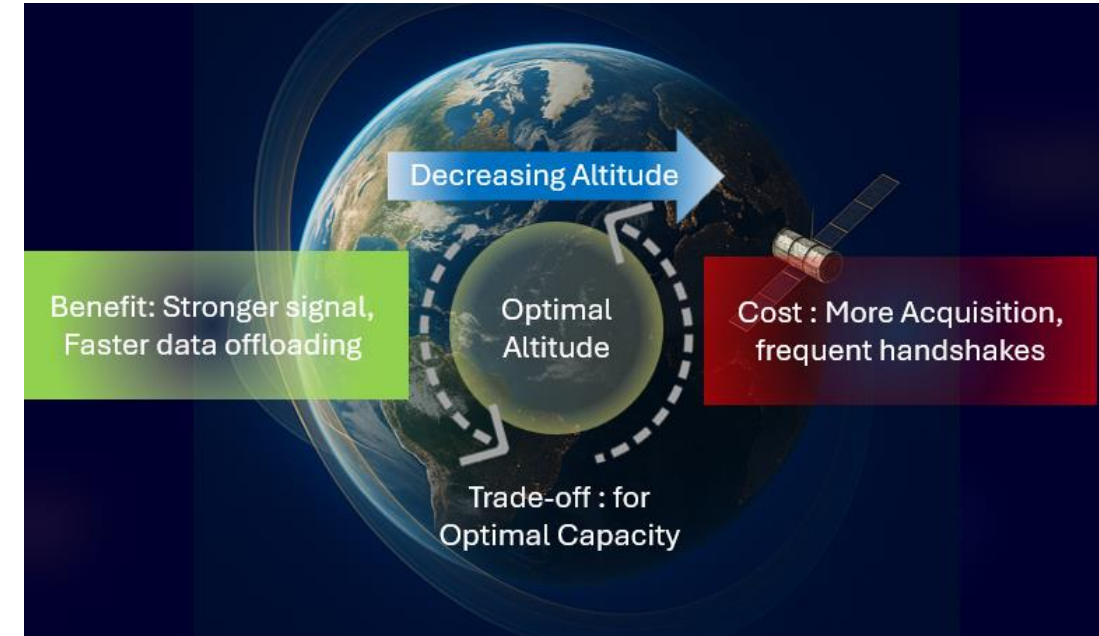


Fig.1 Satellite orbit trade-offs

[1] C. Schieler, B. Robinson, O. Guldner, B. Bilyeu, A. Garg, K. Riesing, J. Chang, F. Hakimi, J. Brown, F. Khatri, et al., "NASA's terabyte infrared delivery (TBIRD) program: Large-volume data transfer from LEO," 2019.

[2] https://www.esa.int/Enabling_Support/Space_Transportation/Types_of_orbits#LEO

◆ Gap

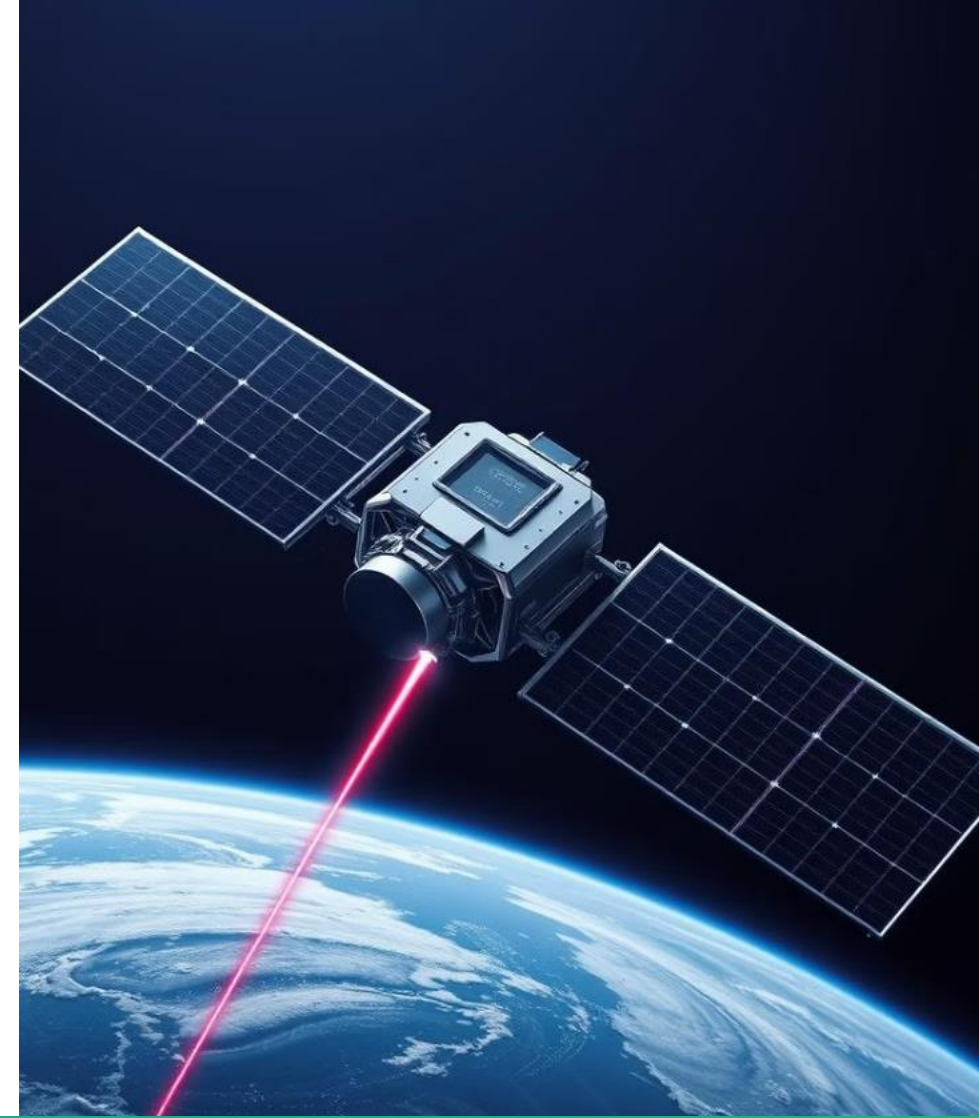
➤ Existing missions (TBIRD, ARCSTONE, OCSD)[1],[3],[4] demonstrate feasibility but lack systematic optimization for jointly selecting:

- Orbit altitude
- Beamwidth
- Transmit power
- Elevation Angle

To maximize average downlink capacity and freshness of information under DTN constraints.

◆ Research Question

- How can we place satellites and choose orbits so that energy transfer windows coincide with the highest-capacity downlinks
- Objective: Maximizing data delivery with minimal loss and delay



[3] Stone, Thomas C. "Acquisition of Moon measurements by Earth orbiting sensors for lunar calibration." IEEE Transactions on Geoscience and Remote Sensing 60 (2021): 1-6.

[4] Rose, Todd S., et al. "Optical communications downlink from a 1.5 U CubeSat: OCSD program." International Conference on Space Optics—ICSO 2018. Vol. 11180. SPIE, 2019.

◆ Orbit Type Selection for LEO Satellites

➤ Circular Orbits:

- Constant altitude, uniform coverage
- Ideal for Earth observation and consistent communication

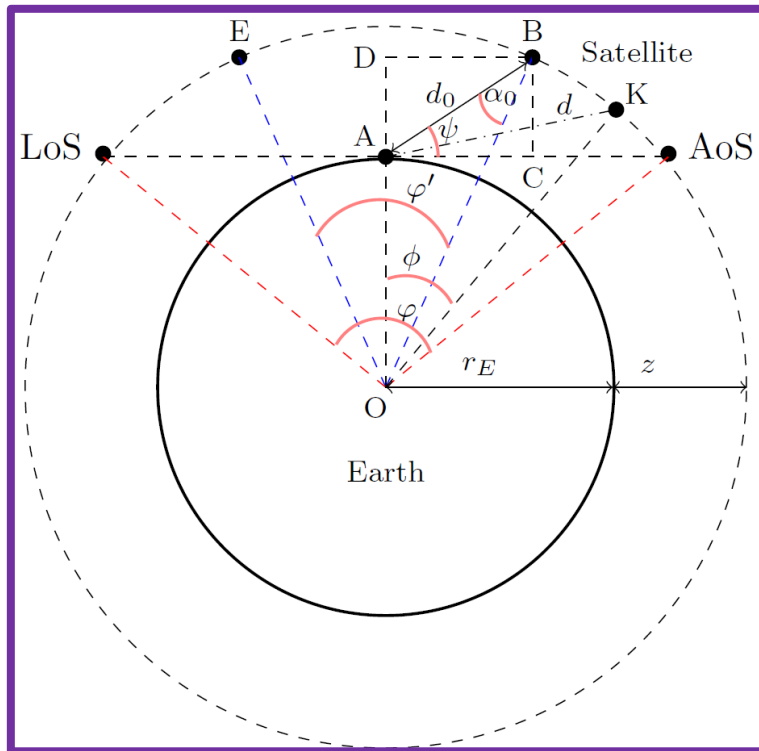


Fig.2 Satellite-Earth geometry of a satellite in circular orbit.

➤ Elliptical Orbits:

- Varying altitude, Prolonged focus over regions
- Suitable for remote sensing, targeted high-latitude coverage

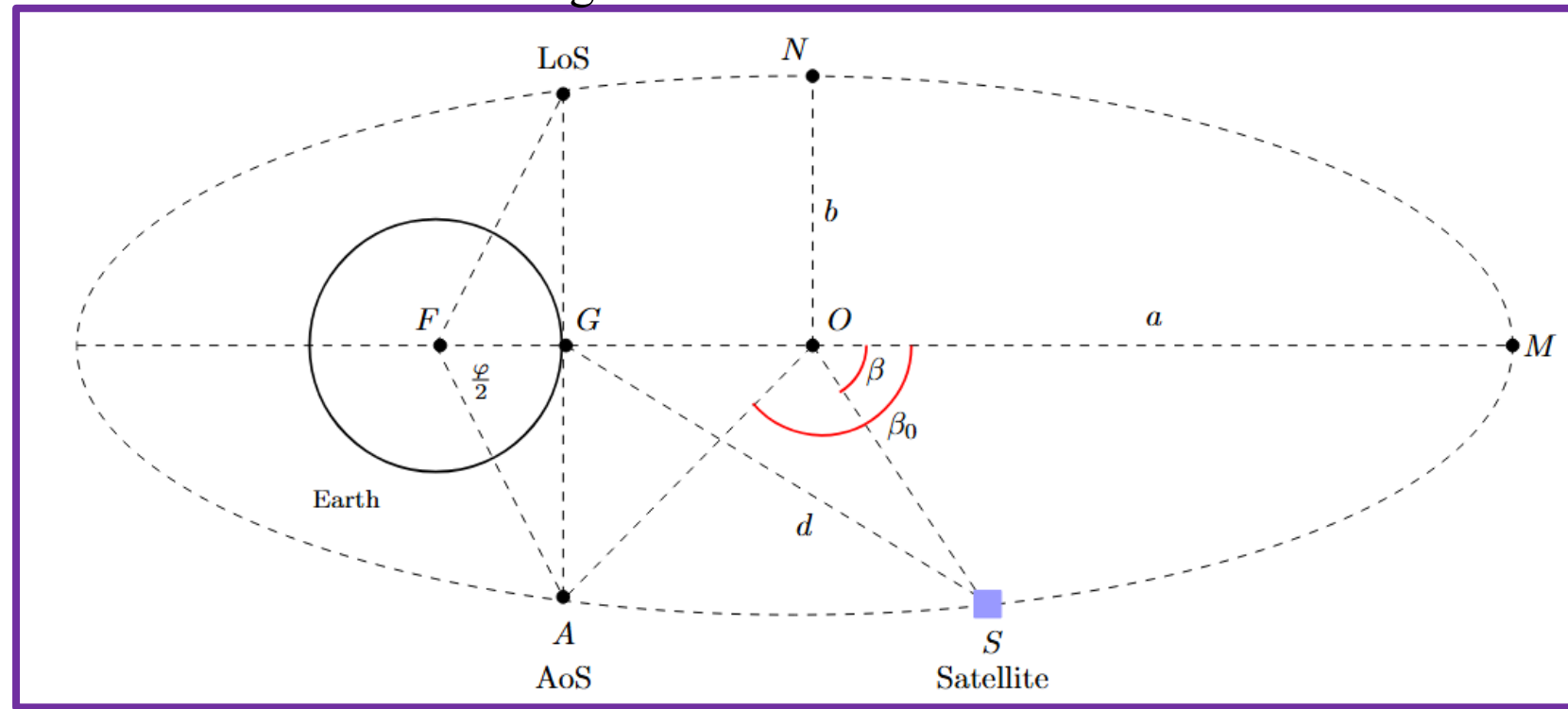


Fig.3 Satellite-Earth geometry of a satellite in elliptical orbit.

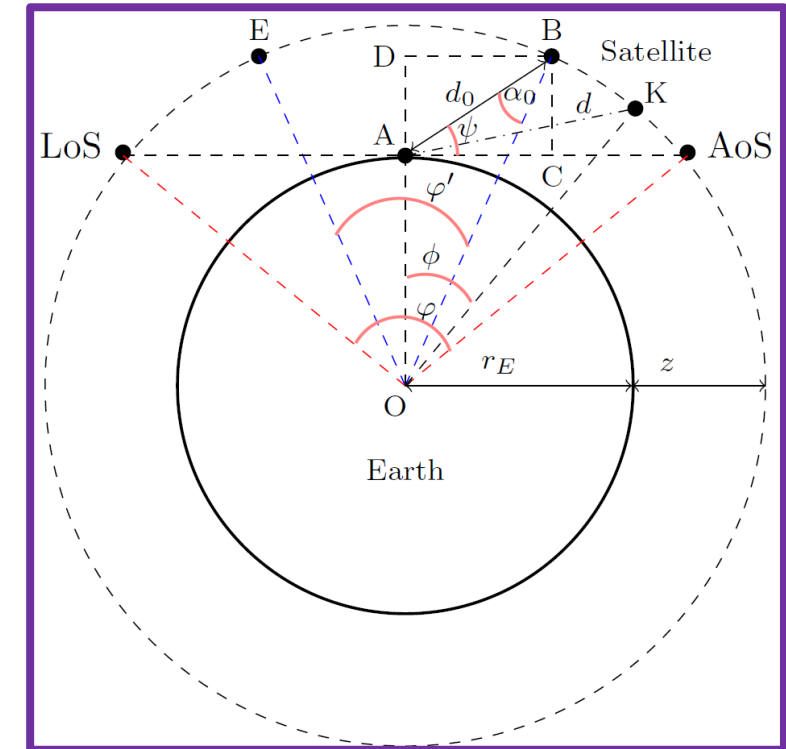
◆ 1. Circular Orbit FSO Channel Analysis

- ✓ In practice, obstructions near the horizon necessitate a minimum elevation angle constraint $\psi > 0$ to maintain reliable line-of-sight communication.
- ✓ Reduces the effective visibility window and thus the link availability

$$\varphi'(\psi) = 2 \left(\arccos \left(\frac{r_E}{r_E + z} \cos(\psi) \right) - \psi \right).$$

$$d_0(\psi) = \sqrt{z^2 + 2zr_E + r_E^2 \sin^2 \psi} - r_E \sin \psi,$$

$$z < d_0 < \sqrt{z(z + 2r_E)}.$$



◆ 1. Circular Orbit FSO Channel Analysis

- ✓ The total signal current flowing out of the detection elements (after photoconversion) is $\mathcal{S} = \eta S(d)$,
- ✓ An upper bound on the normalized instantaneous capacity $\mathcal{C} = \log_2 \left(1 + \frac{\mathcal{S}^2}{\sigma_n^2} \right)$ bits/s/Hz .
- ✓ The maximum amount of data, that can be offloaded to the ground station within one orbital period is $\mathcal{D}(z)$

$$\mathcal{D}(z) = \mathcal{W} \mathbb{E}[\mathcal{C}] = \mathcal{W} \int_{-\varphi/2}^{\varphi/2} \int_0^\infty \log_2 \left(1 + \frac{\left(\eta \frac{2P_t}{2\pi\theta^2 d^2(z, \phi)} \exp \left(-\frac{r^2}{2\theta^2 d^2(z, \phi)} \right) \pi a_{rx}^2 \right)^2}{\sigma_n^2} \right) f_R(r) f(\phi) dr d\phi. \text{ bits/Hz}$$

$$f(\phi) = \frac{1}{\varphi} \cdot \mathbb{1}_{(-\varphi/2, \varphi/2)}(\phi)$$

- ✓ The ergodic capacity for a pointing error dominant channel $C_P(z)$

$\mathbb{1}_A(y)$ is 1 when $y \in A$ and 0 otherwise

$$C_P(z) = \frac{\mathcal{D}}{T} = \frac{1}{2\pi} \int_{-\varphi/2}^{\varphi/2} \int_0^\infty \log_2 \left(1 + \frac{\left(\eta \frac{2P_t}{2\pi\theta^2 d^2(z, \phi)} \exp \left(-\frac{r^2}{2\theta^2 d^2(z, \phi)} \right) \pi a_{rx}^2 \right)^2}{\sigma_n^2} \right) f_R(r) dr d\phi. \text{ bits/s/Hz}$$

◆ Atmospheric Turbulence and Pointing Error Impaired FSO Channel Analysis

- ✓ When the FSO channel is subject to both pointing errors and atmospheric turbulence, the received power can be reproduced

$$\text{as } S(d) = \frac{2IP_t}{2\pi w^2(d)} \exp\left(-\frac{R^2}{2w^2(d)}\right) \pi a_{rx}^2$$

$$f_I(I; \alpha_{GG}, \beta_{GG}) = \frac{2(\alpha_{GG}\beta_{GG})^{\frac{\alpha_{GG}+\beta_{GG}}{2}}}{\Gamma(\alpha_{GG})\Gamma(\beta_{GG})} \\ \times I^{\frac{\alpha_{GG}+\beta_{GG}}{2}-1} K_{\alpha_{GG}-\beta_{GG}}(2\sqrt{\alpha_{GG}\beta_{GG}}I), I > 0$$

- ✓ The ergodic capacity considering both the pointing error and scintillation due to atmospheric turbulence

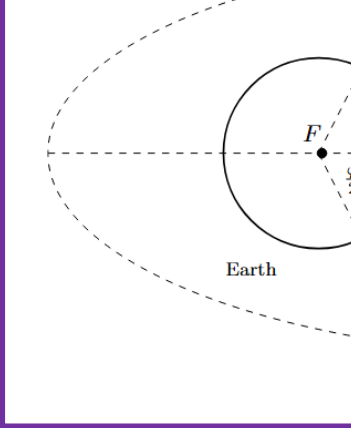
$$C_{PT}(z) = \frac{1}{2\pi} \int_{-\varphi/2}^{\varphi/2} \int_0^\infty \int_0^\infty \log_2 \left(1 + \frac{(\eta \frac{2IP_t}{2\pi \theta^2 d^2(z, \phi)} \exp(-\frac{r^2}{2\theta^2 d^2(z, \phi)}) \pi a_{rx}^2)^2}{\sigma_n^2} \right) f_R(r) f_I(I; \alpha_{GG}, \beta_{GG}) dr dI d\phi.$$

- ✓ Gauss-quadrature (GQ) approximation for smooth integrations with comparable accuracy using far fewer sample points where:

$$C_{PT}(z) \approx \frac{\varphi}{4\pi} \sum_{j=1}^{N_\phi} \sum_{k=1}^{N_I} \sum_{i=1}^{N_r} w_j^{GL} \tilde{w}_k^{GLa} w_i^{GH} \log_2 \left(1 + \frac{A^2(\phi_j, r_i) I_k^2}{\sigma_n^2} \right) |x_i|.$$

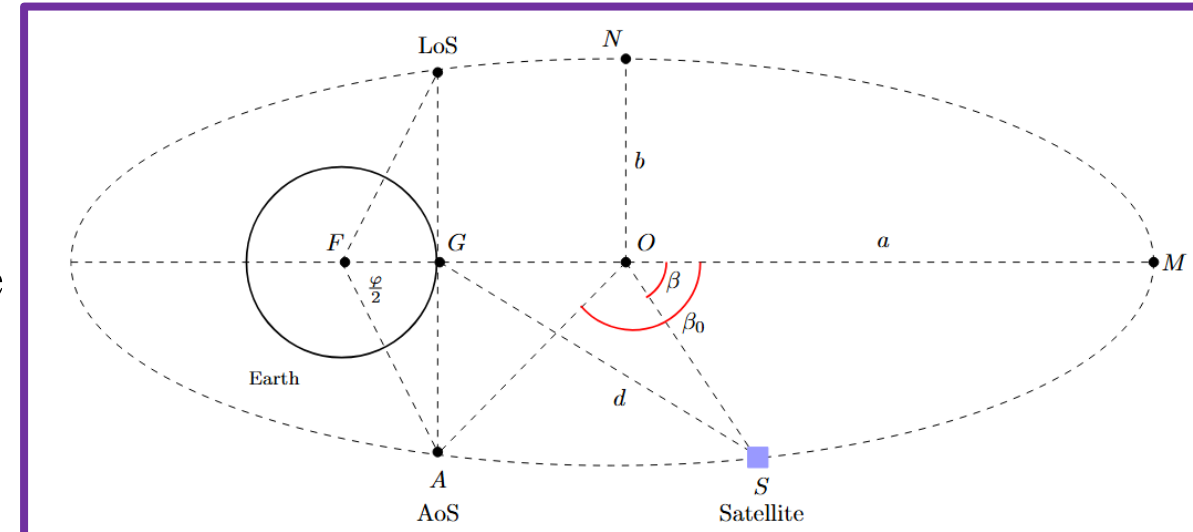
- $\phi_j = \frac{\varphi}{2} t_j$, $r_i = \sigma_R \sqrt{2} |x_i|$, $\tilde{w}_k^{GLa} = w_k^{GLa} f_I(I_k) e^{I_k}$,
- $\{x_i, w_i^{GH}\}_{i=1}^{N_r}$, $\{I_k, w_k^{GLag}\}_{k=1}^{N_I}$, and $\{t_j, w_j^{GL}\}_{j=1}^{N_\phi}$, denote the Gauss-Hermite, Gauss-Laguerre and Gauss-Legendre nodes/weights, respectively.
- N_r , N_I , and N_ϕ are the numbers of quadrature points for the r , I , and ϕ integrals, respectively.

◆ 2. Elliptical Orbit FSO Channel Analysis

- ✓ The eccentricity of the elliptical orbit $\mathcal{E} = \sqrt{1 - \frac{b^2}{a^2}}$
 - ✓ The distance between centre of the Earth and the satellite on the ellipse is $\mathcal{D} = \sqrt{(a \cos(\beta) - \sqrt{a^2 - b^2})^2 + b^2 \sin^2(\beta)}$
 - ✓ The velocity is furnished by $v = \sqrt{\mu \left(\frac{2}{\mathcal{D}} - \frac{1}{a} \right)}$.
 - ✓ The orbital period (in seconds) of the satellite is $T = 2\pi \sqrt{\frac{a^3}{\mu}}$.
 - ✓ capacity due to pointing error impairment at a certain angle β on the ellipse between
- 

$$-\beta_0 \text{ and } \beta_0 \text{ is } \mathcal{C}(\beta) = \int_0^\infty \log_2 \left(1 + \frac{\left(\eta \frac{2P_t}{2\pi\theta^2 d^2(\beta)} \exp \left(-\frac{r^2}{2\theta^2 d^2(\beta)} \right) \pi a_{rx}^2 \right)^2}{\sigma_h^2} \right) f_R(r) \mathrm{d}r.$$

- ✓ The total data transmitted during the visibility window $\mathcal{D} = \int_{-\beta_0}^{\beta_0} dD(\beta) = \int_{-\beta_0}^{\beta_0} \frac{\mathcal{C}(\beta)}{v(\beta)} \sqrt{a^2 \sin^2(\beta) + b^2 \cos^2(\beta)} d\beta$.
- ✓ The average capacity—computed over one revolution of the satellite is $\mathcal{C} = \frac{\mathcal{D}}{T} = \frac{1}{T} \int_{-\beta_0}^{\beta_0} \frac{\mathcal{C}(\beta)}{v(\beta)} \sqrt{a^2 \sin^2(\beta) + b^2 \cos^2(\beta)} d\beta$



$$\text{If } \overrightarrow{GO} > 0, \beta_0 = \pi - \arctan \left(\frac{\|\vec{AG}\|}{\vec{GO}} \right)$$

$$\overrightarrow{GO} < 0, \beta_0 = \arctan \left(-\frac{\|\vec{AG}\|}{\vec{GO}} \right)$$

Optimization Problems

1) \mathcal{P}_0 :

$$\max_{z, \theta} C(z, \theta)$$

$$\text{s.t. } \begin{aligned} &i) z \geq 0 \\ &ii) \theta \geq 0 \end{aligned}$$

The optimum geometry is circular unless an application needs extra dwell time over a specific region.

$$2) \mathcal{P}_1: \max_{a, b} C(z)$$

$$\text{s.t. } i) a > r_E + z_0,$$

$$iii) a > b.$$

$$iii) b > \sqrt{2a(r_E + z_0) - (r_E + z_0)^2}.$$

Maximum capacity = 2.33 bits/s/Hz, which occurs at $\theta = 0.94 \times 10^{-6}$ rad and $z = 1940$ km.

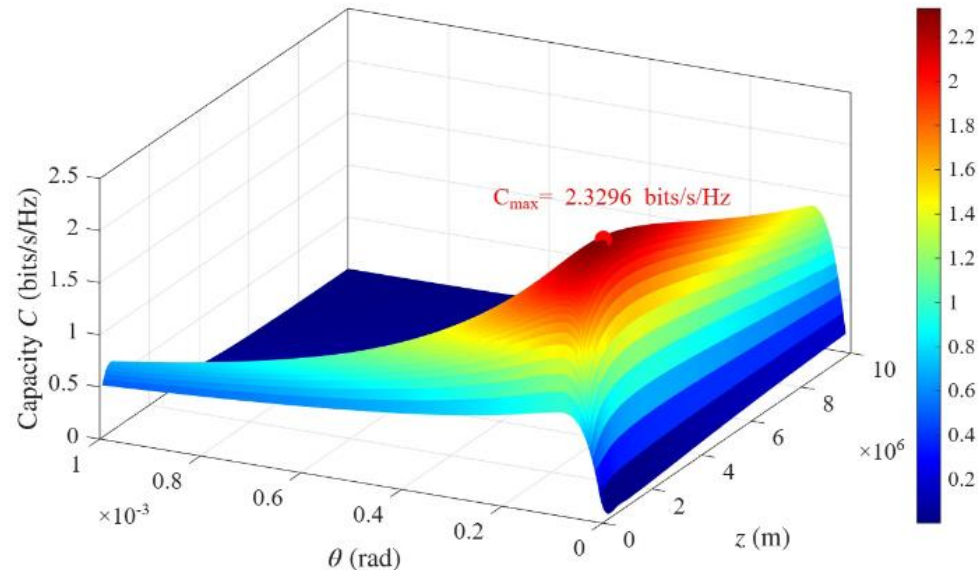


Fig.4 Ergodic capacity in a circular orbit.

- Narrower θ increases both the maximum capacity and the optimal semi-major axis a^*
- Ergodic capacity reaches its maximum when $a=b$

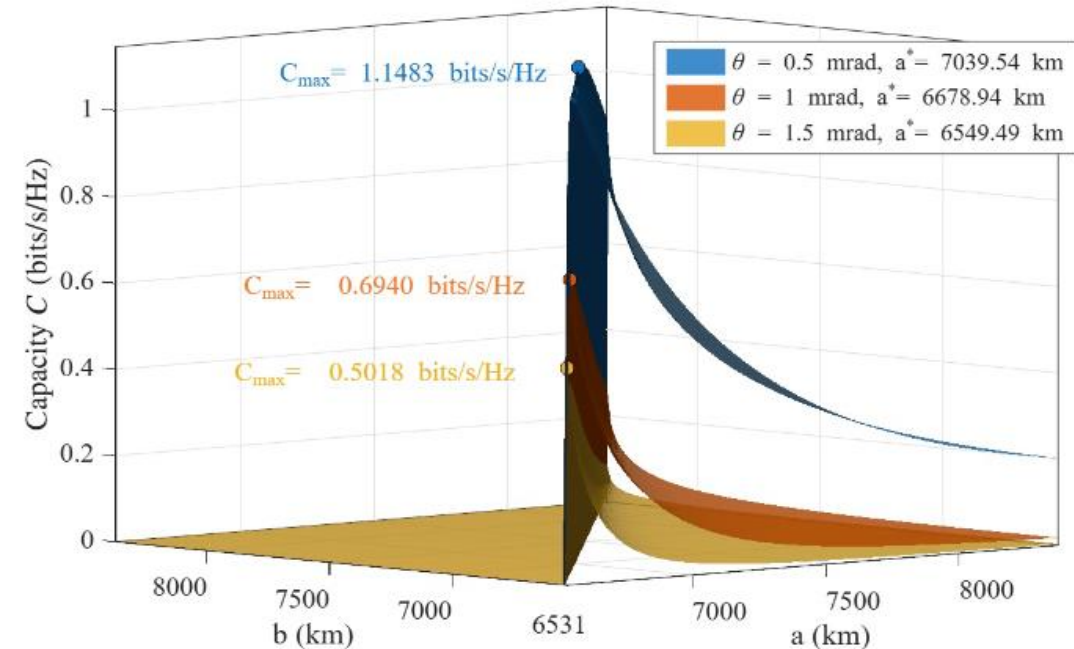


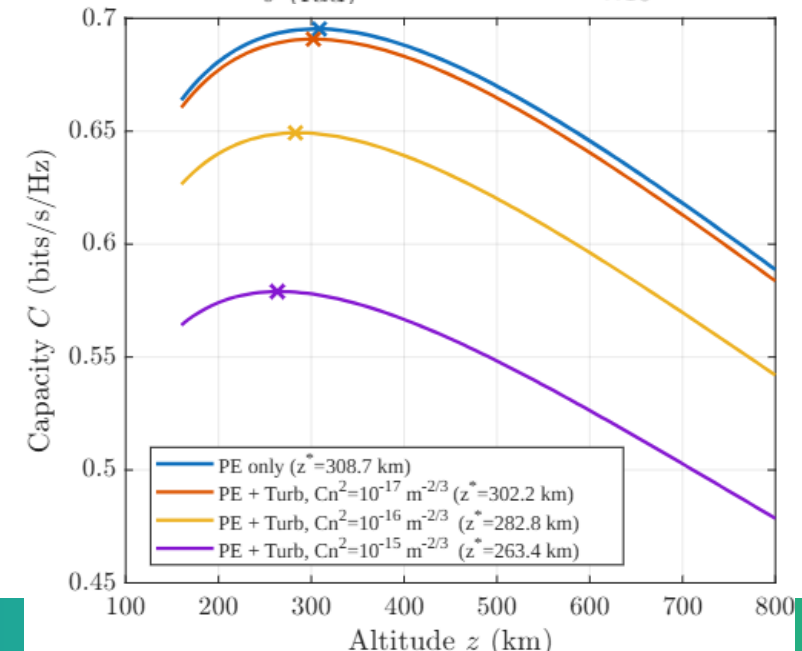
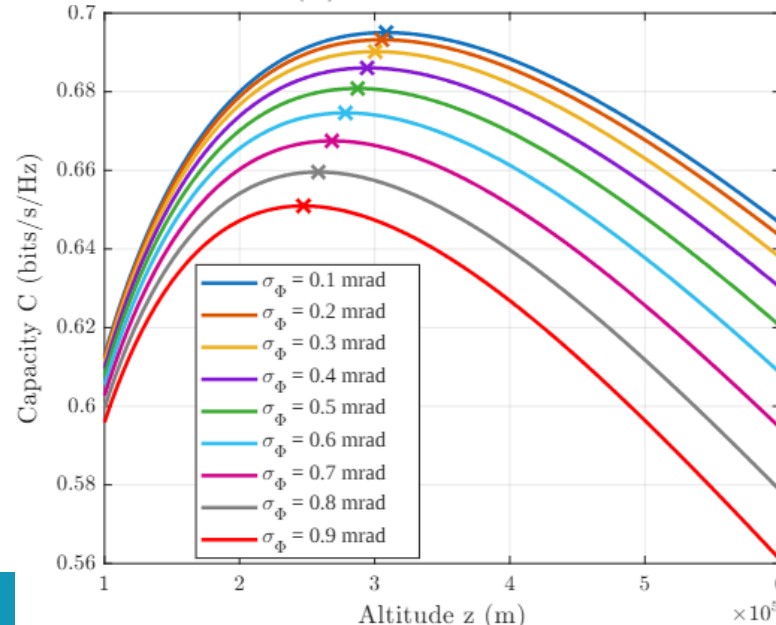
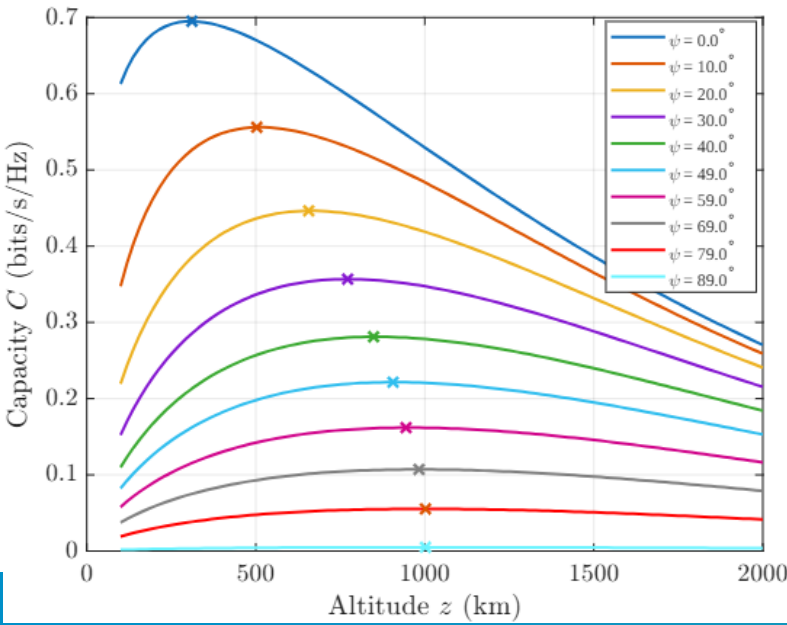
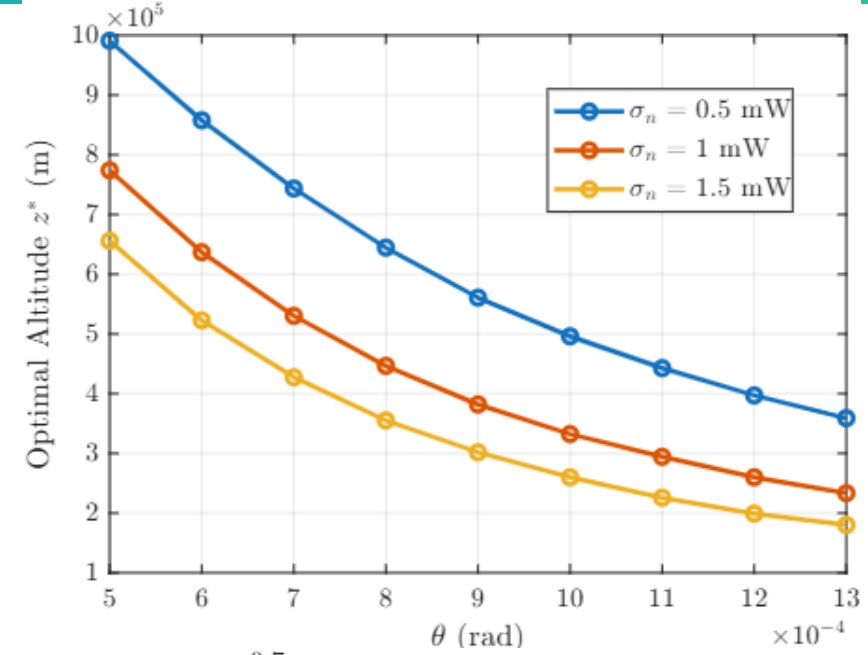
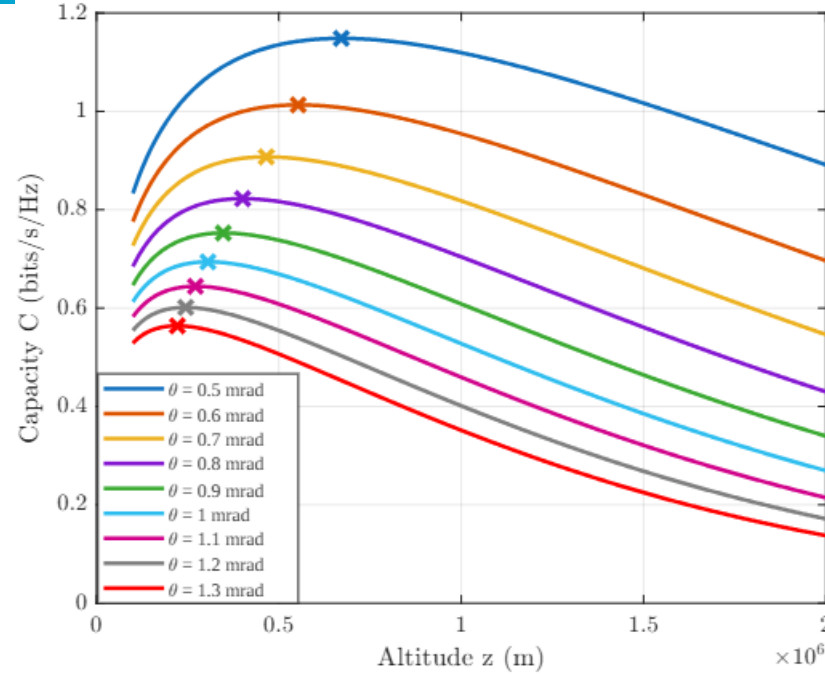
Fig.5 Ergodic capacity in an elliptical orbit.

Circular Orbits

Optimization Problems

3) \mathcal{P}_2

$$\begin{aligned} \max_z \quad & C(z) \\ \text{s.t.} \quad & z > z_0. \end{aligned}$$





UNESCO
Chair on Education

Where to Find Us



جامعة الملك عبد الله
للعلوم والتقنية
King Abdullah University of
Science and Technology



UNESCO
Chair on Education
Connect the Unconnected



LinkedIn



KAUST-CTL Media
YouTube Channel



YouTube



Website



UNESCO
Chair on Education



جامعة الملك عبد الله
للعلوم والتقنية
King Abdullah University of
Science and Technology

Thank You

“

A telephone subscriber here may call up and talk to any other subscriber on the **Globe**. An **inexpensive** receiver, not bigger than a watch, will enable him to listen **anywhere**, on **land** or **sea**, to a speech delivered or music played in some other place, however **distant**.

— Nikola Tesla 1919

UNESCO

Chair on Education Connect the Unconnected

Communication Theory Lab

King Abdullah University of Science and Technology